

1 **Microclimatic edge-to-interior gradients of** 2 **European deciduous forests**

3 Camille Meeussen^a, Sanne Govaert^a, Thomas Vanneste^a, Kurt Bollmann^b, Jörg Brunet^c, Kim
4 Calders^d, Sara A. O. Cousins^{e,i}, Karen De Pauw^a, Martin Diekmann^f, Cristina Gasperini^{g,a}, Per-Ola
5 Hedwall^c, Kristoffer Hylander^{h,i}, Giovanni Iacopetti^g, Jonathan Lenoir^j, Sigrid Lindmo^k, Anna
6 Orczewska^l, Quentin Ponette^m, Jan Plue^c, Pieter Sanczuk^a, Federico Selvi^g, Fabien Spicher^j, Hans
7 Verbeeck^d, Florian Zellweger^b, Kris Verheyen^a, Pieter Vangansbeke^a and Pieter De Frenne^a

8 ^aForest & Nature Lab, Department of Environment, Ghent University, 9090 Melle-Gontrode,
9 Belgium

10 ^bSwiss Federal Institute for Forest, Snow and Landscape Research WSL, 8903 Birmensdorf,
11 Switzerland

12 ^cSouthern Swedish Forest Research Centre, Swedish University of Agricultural Sciences, 234 22
13 Lomma, Sweden

14 ^dCAVElab – Computational and Applied Vegetation Ecology, Department of Environment, Ghent
15 University, 9000 Ghent, Belgium

16 ^eLandscape, Environment and Geomatics, Department of Physical Geography, Stockholm University,
17 10691 Stockholm, Sweden

18 ^fVegetation Ecology and Conservation Biology, Institute of Ecology, FB2, University of Bremen,
19 28359 Bremen, Germany

20 ^gDepartment of Agriculture, Food, Environment and Forestry, University of Florence, 50144
21 Florence, Italy

22 ^hDepartment of Ecology, Environment and Plant Sciences, Stockholm University, 10691 Stockholm,
23 Sweden

24 ⁱBolin Centre for Climate Research, Stockholm University, 10691 Stockholm, Sweden

25 ^jUMR 7058 CNRS « Ecologie et Dynamique des Systèmes Anthropisés » (EDYSAN), Université de
26 Picardie Jules Verne, 80000 Amiens, France

27 ^kDepartment of Biology, Norwegian University of Science and Technology, 7491 Trondheim,
28 Norway

29 ^lInstitute of Biology, Biotechnology and Environmental Protection, Faculty of Natural Sciences,
30 University of Silesia, 40-007 Katowice, Poland

31 ^mEarth and Life Institute, Université catholique de Louvain, 1348 Louvain-la-Neuve, Belgium

32 **Corresponding author:**

33 Camille Meeussen

34 Forest & Nature Lab, Department of Environment, Ghent University, Geraardsbergsesteenweg 267,
35 9090 Melle-Gontrode, Belgium

36 Camille.meeussen@ugent.be

37 Orcid ID:0000-0002-5869-4936

38 Abstract

39 Global forest cover is heavily fragmented. Due to high edge-to-surface ratios in small forest patches,
40 a large proportion of forests is affected by edge influences involving steep microclimatic gradients.
41 Although forest edges are important ecotones and account for 20% of the global forested area, it
42 remains unclear how biotic and abiotic drivers affect forest edge microclimates at the continental
43 scale. Here we report soil and air temperatures measured in 225 deciduous forest plots across Europe
44 for two years. Forest stands were situated along a latitudinal gradient and subject to a varying
45 vegetation structure as quantified by terrestrial laser scanning. In summer, the average offset of air
46 and soil temperatures in forest edges compared to temperatures outside the forest amounted to -2.8°C
47 and -2.3°C , respectively. Edge-to-interior summer temperature gradients were affected by the
48 macroclimate and edge structure. From the edge onwards, larger offsets were observed in dense forest
49 edges and in warmer, southern regions. In open forests and northern Europe, altered microclimatic
50 conditions extended deeper into the forest and gradients were steeper. Canopy closure and plant area
51 index were important drivers of summer offsets in edges, whereas in winter also the forest-floor
52 biomass played a key role. Using high-resolution maps, we estimated that approximately 10% of the
53 European broadleaved forests would be affected by altered temperature regimes. Gradual transition
54 zones between forest and adjacent lands are valuable habitat types for edge species. However, if cool
55 and moist forest interiors are desired, then (i) dense and complex forest edges, (ii) an undisturbed
56 forested buffer zone of at least 12.5 m deep and (iii) trees with a high shade casting ability could all
57 contribute to an increased offset. These findings provide important guidelines to mitigate edge
58 influences, to protect typical forest microclimates and to adapt forest management to climate change.

59 Keywords

60 Climate change, Edge influence, Forest structure, Fragmentation, Temperate forests, Temperature
61 buffering

62 1. Introduction

63 Global temperatures have increased by approximately 1°C in the past century and are expected to rise
64 further (IPCC, 2018). However, at local scales such as in forest stands, worldwide warming trends
65 might be less pronounced and climate-change impacts on forest organisms living in the understory
66 partly dampened (Bertrand et al., 2011; De Frenne et al., 2019; Zellweger et al., 2020). Indeed, the
67 forest microclimate, the local climatic conditions below tree canopies, can differ considerably from
68 the regional climate due to terrain features or vegetation structure and composition (Chen et al., 1999;
69 Geiger et al., 2009), and therefore do not necessarily follow the same trends as regional temperature
70 increases. Due to the shading and evaporation of the vegetation canopy, forest-floor organisms
71 receive less light, less extreme temperatures and thereby a lower temperature variability throughout
72 the day and year in comparison to open areas (Chen et al., 1995; De Frenne et al., 2019; Zellweger et
73 al., 2019). Understorey organisms can even experience an offset which is greater than the warming
74 rates of air temperatures in the past decades (Frey et al., 2016; De Frenne et al., 2019). Considering
75 forest microclimates are therefore important because they ultimately regulate the survival, growth
76 and dispersal of forest-dwelling organisms and affect important forest ecosystem processes such as
77 tree regeneration, and carbon and nutrient cycling (Aussenac, 2000; Riutta et al., 2012; Chen et al.,
78 2018; De Frenne et al., 2021). Moreover, microclimatic conditions determine the community
79 composition and might explain why certain communities lag behind macroclimate and not
80 microclimate warming (De Frenne et al., 2013, 2015; Stevens et al., 2015; Zellweger et al., 2020).

81 Even within forests, large differences in incoming radiation, wind speed and direction, temperature
82 and humidity occur at short spatial scales. Such local gradients in microclimatic conditions are
83 especially pronounced near forest edges. These transition zones between forests and adjacent open
84 land are characterised by strong inflow of warm or cool air, depending on the season and time of the
85 day (Harper et al., 2005; Schmidt et al., 2017). Especially due to steep changes in vegetation structure
86 and composition (Harper et al., 2005; Meeussen et al., 2020), forest edge zones are characterized by
87 environmental gradients that can extend up to 100 m into the forest interior (Harper et al., 2005;

88 Schmidt et al., 2017). For instance, during the summer, temperature and light levels decrease whereas
89 the relative air humidity increases from the edge towards the forest interior (Matlack, 1993; Davies-
90 Colley et al., 2000; Schmidt et al., 2017). This makes transition zones more susceptible to temperature
91 extremes and drought stress in comparison to forest interiors. Altered microclimatic conditions in
92 forest edges, from warm and dry at the edge to cool and moist in the interior, consequently create
93 gradients in understorey biodiversity and induce the establishment of typical habitats for edge-loving
94 vegetation and organisms (Magura, 2002; Ries et al., 2004; De Smedt et al., 2019; Govaert et al.,
95 2020; De Pauw et al., 2021). Furthermore, they change ecosystem functioning and the provisioning
96 of services such as carbon stocks and cycling (Remy et al., 2016; Meeussen et al., 2021). Forest
97 microclimates have long been studied (Geiger et al., 2009; Schmidt et al., 2019), however, we still
98 lack an assessment of the relative importance of local and regional drivers on the spatiotemporal
99 variation of forest edge microclimates at the continental scale.

100 As a result of large-scale fragmentation, more than 20% of the global forest surface is situated within
101 100 m of a non-forested matrix (Haddad et al., 2015). In Europe alone, the cumulative edge length of
102 broadleaved forests amounts to 9.4 billion metres (Meeussen et al., 2021). A substantial extent of the
103 forested area in Europe is thus subject to strong edge influences and consequently to environmental
104 and ecological gradients penetrating deep into the interior of fragmented forest patches. Such edge
105 influences, and their magnitude and depth of influence, are hitherto difficult to quantify as they can
106 vary across the globe due to factors such as forest structure and composition (i.e. deeper edge
107 influences in more open canopies) and macroclimate (i.e. stronger offsets in warmer climates)
108 (Aussenac; 2000; De Frenne et al., 2019; Lembrechts and Lenoir, 2019). Therefore, it is important to
109 gather information on how the drivers of edge-to-interior microclimatic gradients vary at a continental
110 scale.

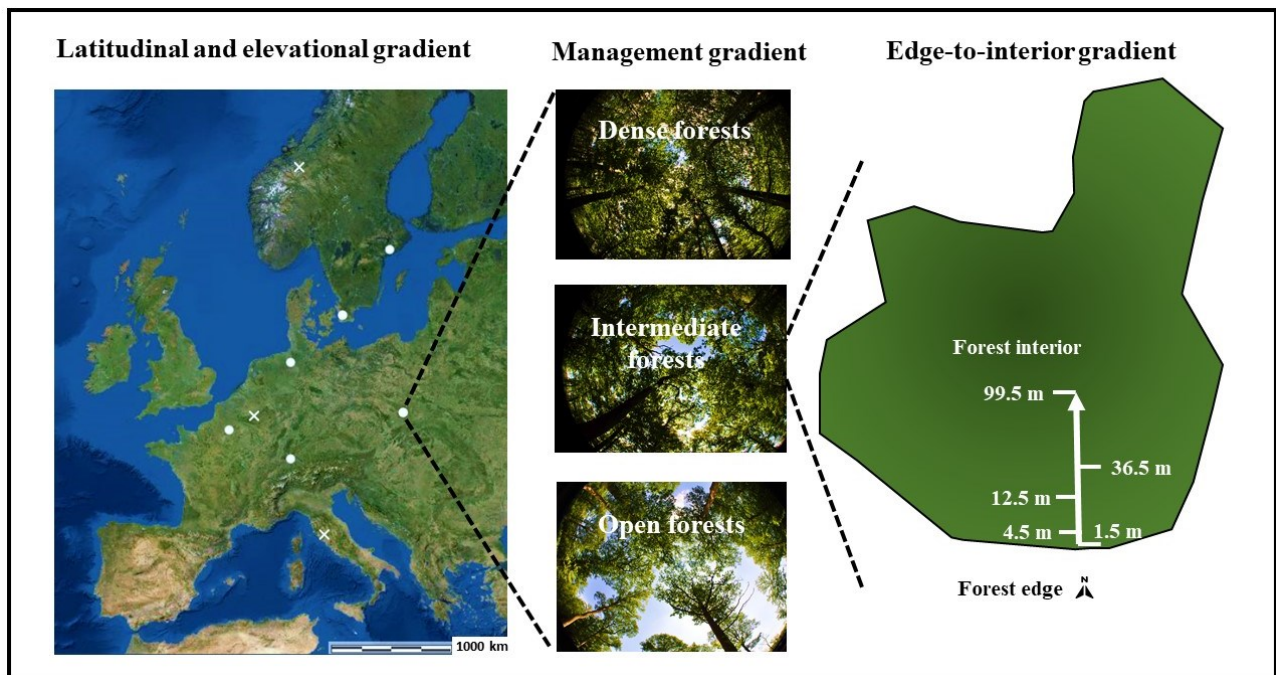
111 Here we assessed air and soil temperature offsets and integrated cumulative evaporation (as a proxy
112 for relative air humidity) in 225 plots in 45 European deciduous forest edges for two years. The forests
113 differed in vegetation structure and complexity, and were situated along a latitudinal gradient from

114 the Mediterranean to central Norway, crossing eight different countries. This study design enabled us
115 to quantify the effect of macroclimate and edge structure on the spatiotemporal variation in
116 microclimatic temperature offsets and evaporation from the edge of the forest towards the interior.
117 We hypothesized to find strong gradients in temperature and evaporation as one moves away from
118 the edge. Moreover, we expected temperature offsets to be strongest in warm, southern European
119 regions and in forests with a dense edge structure, and to find effects of management and
120 macroclimate on the edge-to-interior gradients in temperature. Secondly, to gain a more complete
121 understanding of these patterns, we quantified the influence of several regional (landscape and
122 macroclimatic) characteristics and local site conditions (i.e. forest structure, soil texture and forest-
123 floor litter and humus biomass). In particular, we expected that vegetation structure would play an
124 important role on the forest microclimate, especially during the summer, enabling us to provide
125 guidelines on how to protect forest interior microclimates.

126 2. Material and Method

127 2.1 Study design

128 Data were collected in 45 ancient mesic deciduous forests, mainly dominated by oaks (*Quercus robur*,
129 *Q. petraea* or *Q. cerris*), with *Fagus sylvatica*, *Betula pubescens*, *Populus tremula*, *Ulmus glabra*,
130 *Alnus incana* and *Carpinus betulus* as other (sub)dominant tree species. The stands were situated
131 along a 2300 km long south-north gradient across Europe. Along this latitudinal gradient, nine regions
132 were selected from Central Italy up to Central Norway, covering a mean annual temperature
133 difference of approximately 13°C (**Figure 1**). In three of the nine regions, Norway, Belgium and Italy,
134 an additional elevational gradient with three levels (i.e. low, intermediate and high elevational sites)
135 was established as well to capture climatic variation resulting from elevational differences (expected
136 temperature difference $\approx 5.76^\circ\text{C}$; ICAO, 1993). In total, 15 sites (i.e. nine lowland, three intermediate
137 and three high-elevational sites) were selected across Europe.



138
139 **Figure 1:** Overview of the study design with the macroclimatic gradients (latitude and elevation) and forest structural gradients
140 (management and distance to the edge). Left: The nine regions (Central Italy, Northern Switzerland, Northern France, Belgium,
141 Southern Poland, Northern Germany, Southern Sweden, Central Sweden and Central Norway) along the latitudinal gradient, including
142 three additional elevational gradients (shown as white crosses on the map). Background map from: <http://databasin.org>. Middle: The
143 three forest management types. Right: An example of a 100 m-long edge-to-interior gradient, whereby the forest edge is defined as the
144 outermost line of tree trunks bordering the non-forested matrix. The forest interior is the forest area not characterized by edge

145 influences, where abiotic and biotic conditions thus stay relatively homogenous. Figure after Meeussen et al. (2021), reproduced with
146 permission.

147 In all sites ($n = 15$), three forest stands were selected with a different structure and management type
148 (**Figure 1**). The first type, referred to as ‘dense forests’, were always the most structurally complex
149 stands. They had not been thinned for at least three decades or managed in the past ten years, and
150 therefore comprised of a dense canopy (canopy openness $< 10\%$), high basal area ($> 20 \text{ m}^2$ per ha)
151 and a well-developed shrub layer. Intermediate forests, the second management type, were stands
152 with a lower basal area ($10\text{-}25 \text{ m}^2$ per ha) and higher openness ($5\text{-}30\%$), resulting from regular but
153 not too recent (at least five to ten years before sampling) thinning events. The third and final
154 management type represented ‘open forests’. These stands were even-aged with a simple structure
155 without shrubs and a subdominant tree layer as they were intensively thinned one up to four years
156 before sampling. Where possible, they were selected based on a low canopy openness ($30\text{-}50\%$) and
157 low basal area ($< 10\text{-}15 \text{ m}^2$ per ha). Further details on the study design, forest structure and site
158 selection can be found in Govaert et al. (2020), Meeussen et al. (2020, 2021), De Pauw et al. (2021)
159 and Sanczuk et al. (2021) as this paper is part of larger research project with a common same study
160 design.

161 In each of the 45 forest stands, we studied a 100 m-long gradient perpendicular to the forest edge
162 (**Figure 1**). The edges all bordered a matrix of agricultural land and were approximately south-
163 oriented. Edge orientation was kept constant, because of its known impact on microclimate and depth
164 of edge influence through exposure to direct radiation (Matlack, 1993; Chen et al., 1995; Murcia,
165 1995). Along each edge-to-interior gradient, five 3 m by 3 m plots were established at predefined
166 distances from the forest edge towards the core following an exponential curve ($n = 225$), as the
167 strongest changes in microclimatic conditions were expected to occur near the forest edge. The centre
168 of the first plot was situated at a distance of 1.5 m from the edge, a second plot was located at 4.5 m
169 from the edge and three more plots were centred at 12.5 m, 36.5 m and 99.5 m from the edge (**Figure**
170 **1**). The fifth plot, situated at approximately 100 m from the forest edge, was considered representative

171 of the forest's interior, a presumption in line with other studies finding the macroclimatic edge
172 influences to dissipate within such a distance (Matlack, 1993; Young and Mitchell, 1994; Davies-
173 Colley et al., 2000; Schmidt et al., 2017).

174 2.2 Data collection

175 2.2.1 Microclimatic data

176 We measured air and soil temperatures during two full years, from 1 June 2018 to 31 May 2020. Both
177 air and soil temperatures were recorded at hourly intervals in each plot, using lascar temperature
178 loggers (EasyLog EL-USB-1, accuracy at -35 to +80°C: $\pm 0.5^{\circ}\text{C}$). Air temperatures were measured
179 at a height of 1 m above the forest floor. The sensors were attached to the north side of a wooden
180 pole, which was placed in the centre of each plot, and were protected by plastic white radiation shields
181 to avoid direct solar radiation on the sensors (**Supplementary figure A1**). For the soil temperature,
182 we buried the loggers horizontally in the ground in a protective plastic tube at a depth of 5 cm and 5
183 cm next to the wooden poles (**Supplementary figure A1**). This set-up, the combination of the pole
184 with air and soil data logger, was installed in each plot ($n = 450$ sensors) and repeated outside the
185 forest for each of the fifteen sites ($n = 30$ reference sensors). The latter to quantify fully open
186 conditions outside the forest to obtain reference macroclimate conditions not influenced by the forest
187 canopy. All these 30 reference sensors (i.e. one soil and one air data logger per site) were installed in
188 open grasslands in the vicinity (generally within a radius of 5 km) of the respective forest edges.

189 After data collection, time series were visually checked for outliers (e.g. due to uprooting of the soil
190 loggers by wild boar, broken radiation shields and poles) by plotting and comparing them with the
191 other time series of sensors within the same site or the reference sensors. Biased temperature
192 measurements, showing deviating trends or clear outliers, were removed from the dataset and
193 subsequently daily minima, maxima and mean temperatures were determined for each sensor. Next,
194 we calculated the daily mean (T_{mean}), minimum (T_{min}) and maximum (T_{max}) temperature offset,
195 which corresponds to the temperature difference between each of the temperature loggers located
196 along the edge-to-interior gradient and the reference temperature logger located in open conditions
197 (offset = edge-to-interior gradient location minus open reference location). Negative offsets thus

198 depict cooler conditions inside the edge-to-interior gradient than in the open reference location, and
199 vice versa. Finally, our daily temperature offset values were aggregated into monthly averages, and
200 afterwards seasonal offsets (spring: March, April and May; summer: June, July and August; autumn:
201 September, October and November; winter: December, January and February), if at least 50% of the
202 data were available for that month/season. In the best case, we obtained 225 offset values (one per
203 plot) for Tmean, Tmin and Tmax for both soil and air and during each season. To proceed, we mainly
204 focused on the offset during winter and summer, as these seasons show the most contrasting patterns
205 (**Figure 2 and Supplementary figure B1**). Due to missing data, we were unable to calculate the
206 summer air offsets in 2 plots, and the summer and winter soil offsets in 22 and 7 out of the 225 plots,
207 respectively, due to for instance logger malfunctioning or the uprooting of soil sensors.

208 To quantify air humidity integrated over a longer time period, custom-built evaporimeters were
209 installed in May-June 2018. These evaporimeters were narrow 50 cm long plastic tubes (diameter 14
210 mm), cautiously sealed at the top with a plastic plug and at the bottom with an open cap covered by
211 filter paper (Rotilabo®-Blotting papers, thick. 1.0 mm), functioning as Piche evaporimeters
212 (Papaioannou et al., 1996). The tubes were filled with *c.* 75 mL distilled water, weighted and carefully
213 attached to the wooden pole with tape, at the north side and in such a manner that the tube hung
214 vertically with its lower end 10 cm above the ground. After one month, the tubes were collected and
215 again weighed to determine the water loss. The weight loss was finally converted to water evaporation
216 in mm per week and served as a metric for the integrated, cumulative air humidity inside the forest
217 over this period. Due to damaged filter paper in 24 tubes, 201 of the 225 measurement points were
218 available for further analyses.

219 *2.2.2 Explanatory variables*

220 *Local site characteristics*

221 *Forest structure and composition*

222 The forest structure was quantified between May and July 2018. Primarily, we visually estimated the
223 vertical species-specific cover of all shrub (1-7 m) and tree species (> 7 m) in the 3 by 3 m plots. The
224 average shade casting ability (SCA) was determined per plot, based on the SCA-score of individual

225 trees and shrubs weighted by their respective cover. The SCA is an expert-based and species-specific
226 index, ranging between 1 and 5, describing the ability of trees and shrubs to cast low levels of shade
227 (SCA close to one e.g. *Betula pendula*) or high levels of shade (SCA close to five e.g. *Fagus sylvatica*)
228 (Verheyen et al., 2012). Species-specific SCA-scores were obtained from the literature (i.e. Verheyen
229 et al., 2012 and Govaert et al., 2020) and are listed in the appendix (**Table A1**). Subsequently, in
230 every plot, a larger circular plot with a 9 m radius was established. In these plots, the average diameter
231 of all trees with a diameter at breast height (DBH, 1.3 m) larger than 7.5 cm were determined via two
232 DBH measurements per stem, perpendicular to each other, using a caliper. Subsequently, we
233 calculated the total basal area per hectare at plot level. Next, we used terrestrial laser scanning (TLS)
234 to further map the complex three-dimensional structure of the forest (Calders et al., 2020); all
235 technical details considering this campaign are described in Meeussen et al. (2020). Single-scan
236 position TLS was carried out in the centre of the plots using a RIEGL VZ400 (RIEGL Laser
237 Measurement Systems GmbH, Horn, Austria). Based on the scans, we derived four more forest
238 structural metrics. Firstly, we determined the plant area index, a metric for plant material density or
239 the total of the one-sided area of woody (e.g. branches) and non-woody biomass (i.e. leaves) per unit
240 of surface area. More specifically, the plant area index was computed as the integral of the plant area
241 per volume density (PAVD, $\text{m}^2 \text{m}^{-3}$) over the canopy top height. The plant area index of the shrub
242 layer, as second metric, was determined as the total PAVD below a height of 7 m. Thirdly, we
243 determined the canopy top height, based on the 99% PAVD-percentile to remove atmospheric noise.
244 Lastly, as a fourth TLS-derived metric, canopy closure was used. Canopy closure is the complement
245 of canopy openness, which was calculated as the average percentage of gap fraction, the probability
246 of a beam to miss all scattering elements in the forest (i.e. foliage or wood) and escape through the
247 canopy, across the angle 5-70°.

248 *Forest-floor biomass and soil texture*

249 In addition, two more local site characteristics potentially affecting the forest microclimate were
250 determined: the mass of the forest floor (i.e. litter and humus) and the soil texture (Paul et al., 2004;
251 Fekete et al., 2016; Dutta et al., 2018). In each plot, one random sample of the forest floor, the organic

252 material (i.e. O-horizon(s)) on top of the mineral topsoil, was taken in a 20 cm by 20 cm square frame
253 after removal of live understorey vegetation. The litter and humus layers were sampled and weighed
254 after drying to constant weight for 48 hours at 65°C to determine the biomass of the forest floor (kg
255 m⁻²). Five subsamples of the soil were taken (10-20 cm depth) in each plot as well. The subsamples
256 were pooled per layer and dried to constant weight at 40°C for 48 hours. Texture analysis was
257 performed by sieving and sedimentation with a Robinson–Köhn pipette according to ISO 11277
258 (2009). We selected the percentage sand (%) as most important proxy for the soil texture's influence
259 on microclimate.

260

261 *Regional characteristics*

262 *Macroclimate temperature and precipitation*

263 Macroclimatic data were obtained from our reference sensors. For every site, we calculated the mean
264 annual temperature (MAT, °C, over the period 1 June 2018 to 31 May 2020) based on the data of the
265 reference air sensors placed in the neighbourhood of our transects. Moreover, to obtain a more exact
266 characterisation of the macroclimate during summer and winter, we also computed the mean seasonal
267 temperature (MST, °C) during winter and summer for both soil and air reference sensors. For each
268 plot, data on the mean total annual precipitation (MAP, mm year⁻¹) were extracted from CHELSA
269 (version 1.2, average climatic conditions over the period 1979-2013 at a spatial resolution of 30 arc
270 sec, Karger et al., 2017). We also performed a sensitivity analysis using gridded macroclimate data
271 (ERA5-Land hourly data, (Muñoz Sabater, 2019)) as reference data instead of our own open-habitat
272 reference sensors. These sensitivity analyses confirm the robustness of our main findings and are
273 available in **Appendix C**.

274 *Landscape structure*

275 Four landscape characteristics were extracted using satellite-based global tree cover data (spatial
276 resolution of 30 m, Hansen et al., 2013), a pan-European digital elevation model (spatial resolution
277 of 25 m), Copernicus data and information from the European Union (EU-DEM, 2018). The
278 percentage of forest cover (%), forests defined as surface areas with a minimum tree cover of 20 %)
279 surrounding each plot was calculated using a circular buffer area with a 500 m radius (Hansen et al.,

280 2013). Topographic northness and slope (°) were derived from the digital elevation model. The
281 topographic northness, derived as the cosine of topographic aspect, represents the topographic
282 exposition and ranges from north facing (+1) to completely south facing (-1). Finally, also distance
283 to the nearest coast was considered as a predictor of the microclimatic offset, as an increased
284 temperature range and reduced air-mixing farther from the coast might affect the offset.

285 2.3 Data analysis

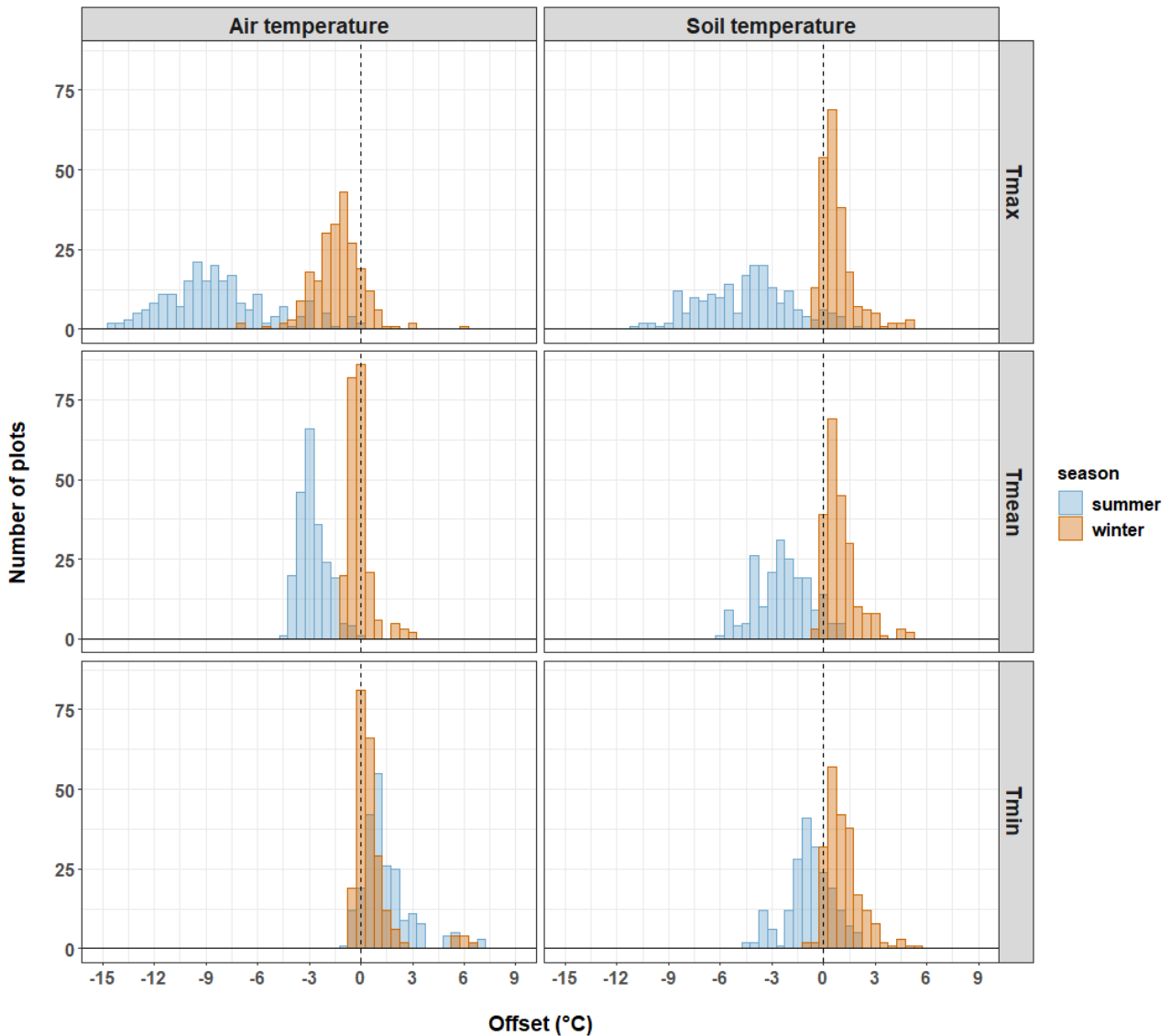
286 Variation in microclimatic gradients in forest edge zones across Europe was analysed in R version
287 4.0.3 (R Core Team, 2020) making use of linear mixed-effect models (Zuur et al., 2009) and the
288 ‘*lmer*’ function in the R-package ‘*lme4*’ (Bates et al., 2015). In all models, region and transect nested
289 within region were added as random effect terms (i.e. random intercepts) to account for the nested
290 structure of our design; plots nested in transects, nested in regions. In a first set of models, we studied
291 the impact of distance to the edge, management type and the macroclimate (MAT, as a continuous
292 variable for region and elevation) (i.e. our fixed effects) on the forest edge microclimate (n ~ 225 for
293 the (winter and summer) air and soil temperature offset, and n = 201 for the evaporation during the
294 summer). Two-way interactions between fixed effects were allowed. Non-significant (interaction)
295 effects were removed from the model during model selection using the ‘*step*’ function of the R-
296 package ‘*lmerTest*’ (Kuznetsova et al., 2017). After model selection, restricted maximum likelihood
297 was employed to assess the model parameters. Distance to the edge was log-transformed prior to
298 analyses since the distribution of our plots followed an exponential pattern and one of the response
299 variables, evaporation, had a right-skewed distribution and was log-transformed as well. If distance
300 to the edge was a significant driver of the microclimate, a post hoc (Tukey Multiple Comparisons)
301 test was executed using the ‘*glht*’ function (‘*multcomp*’ R-package) to explore up to which edge
302 distance (here as a factor, significance level $p < 0.05$) the microclimate differed from the microclimate
303 in the forest interior (i.e. at a distance of 99.5 m from each edge) (Hothorn et al., 2008). This way we
304 determined the depth of edge influence, and subsequently calculated, as a basic and explorative
305 analysis, the percentage of European deciduous forests affected by edge influences in Europe based
306 on the cumulative length of deciduous forest edges across Europe (Meeussen et al., 2021).

307 To achieve a more mechanistic understanding of the microclimate patterns and their drivers, an
308 additional set of models was constructed. Here, the fixed effects were our local site features (shade
309 casting ability (SCA), basal area, plant area index, plant area index of the shrub layer, canopy height,
310 canopy openness, forest-floor biomass and soil texture) and regional landscape and macroclimatic
311 characteristics (seasonal temperature (MST) from the reference sensor, precipitation (MAP), slope,
312 northness, forest cover, and distance to the coast), whereas the random effects stayed the same
313 (transect nested within region). Regarding MST, we always selected the macroclimatic temperature
314 of the same type (air/soil) and same season (winter/summer) as the respective offset metric. For
315 evaporation, the summer macroclimatic air temperature of the reference sensor was used. All
316 continuous predictor variables were standardized to allow for a better comparison of model
317 coefficients. No interaction terms were tested in these models (to make the models not overly
318 complex), and again backward model selection was executed on this second set of models. Also,
319 multicollinearity was tested making use of the variance inflation factor. Multicollinearity among the
320 predictor variables in all models was low (variance inflation factors lower than 3).

321

322 3. Results

323 The average air temperature offset in summer across all plots and transects amounted to $-2.8 \pm 0.8^\circ\text{C}$
 324 whereas in winter the average offset fluctuated around zero ($-0.1 \pm 0.7^\circ\text{C}$). Maximum summer air
 325 temperatures were on average $8.3 \pm 3.1^\circ\text{C}$ cooler inside than outside forests, in contrast, minimum
 326 summer air temperatures were warmer ($1.5 \pm 1.5^\circ\text{C}$) in the forest. Forest soil offsets were on average
 327 $-2.3 \pm 1.6^\circ\text{C}$ during the summer months, with a more negative offset for maximum temperatures ($-$
 328 $4.5 \pm 2.7^\circ\text{C}$) and minimum temperature offsets close to zero ($-0.8 \pm 1.3^\circ\text{C}$). In winter, mean, minimum
 329 and maximum soil temperatures were warmer inside than outside forests (respectively $1.0 \pm 1.0^\circ\text{C}$,
 330 $1.1 \pm 1.0^\circ\text{C}$ and $0.8 \pm 1.0^\circ\text{C}$) (**Figure 2**). The average summer evaporation amounted to 20.06 mm
 331 per week (range: 2.4 – 112.75 mm per week, **Supplementary figure B2**).



333 **Figure 2:** Summary of the seasonal variation in air and soil temperature offsets (°C) for maximum (Tmax), mean (Tmean) and
 334 minimum (Tmin) temperatures for all 225 study plots. Negative offsets indicate cooler temperatures inside forest edge zones.

335
 336 Besides seasonal fluctuations, the offset also depended on the macroclimate, management and
 337 distance to the edge (log-transformed). For almost all offset metrics, except for the offset of the
 338 minimum winter temperature in the forest soil, we found a significant main impact of the distance to
 339 the edge (**Table 1, and Supplementary tables B1 and B2**) or edge distance interactions with MAT
 340 or forest type. In general, these trends indicated an enhanced cooling of mean and maximum
 341 temperatures (i.e. more negative offset) from the forest edge towards the interior during the summer
 342 (**Figure 3A and 3B**), but in winter, higher mean and maximum temperatures (i.e. more positive
 343 offsets) were detected near the edge in comparison to the interior (**Figure 4**). Moreover, we found an
 344 indication of a decreased evaporation in the interior, shown by the significant negative impact of the
 345 distance to the edge on the evaporation (**Figure 3C**).

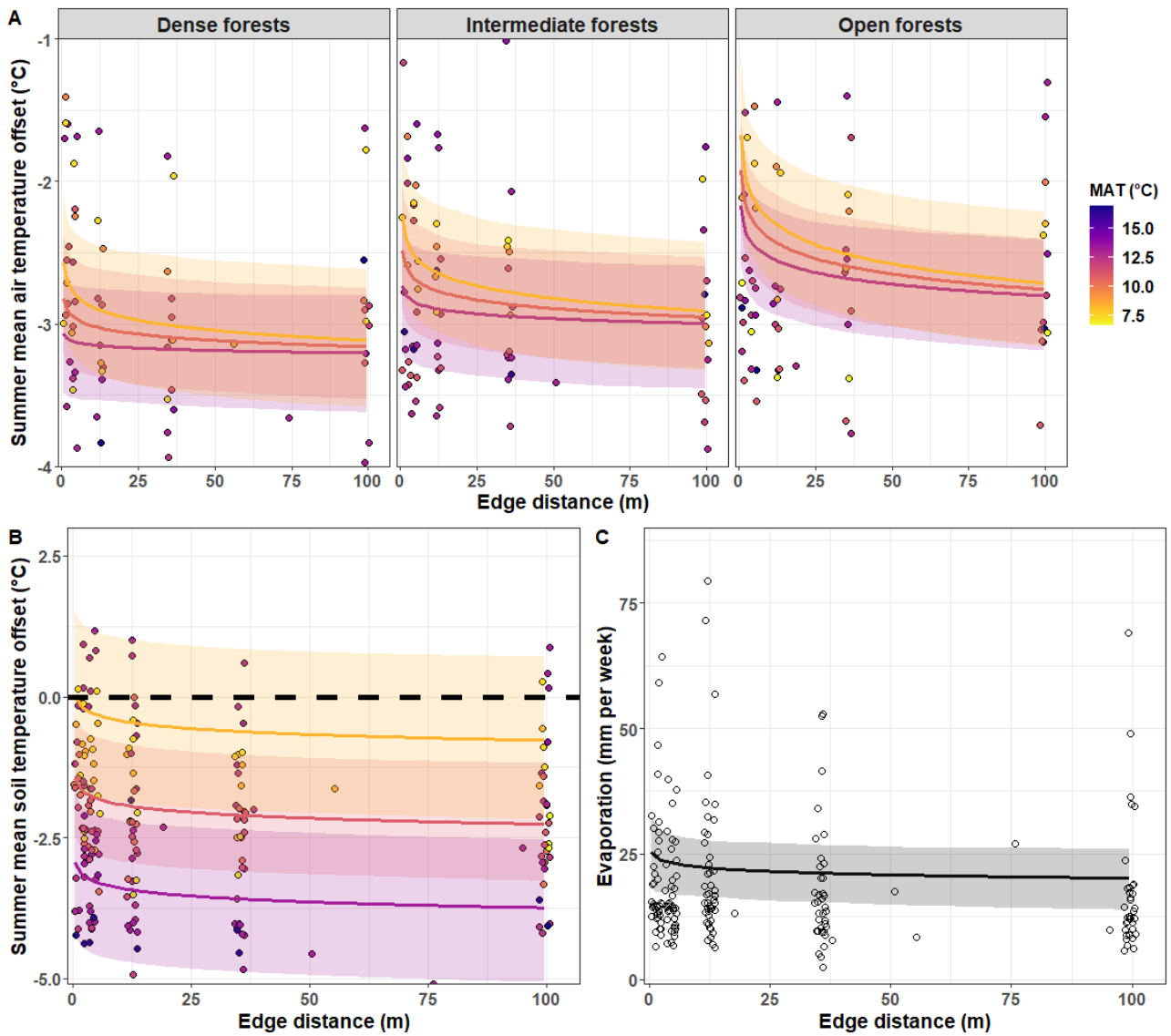
346 **Table 1:** The impact of the design variables (mean annual temperature (= MAT), forest management type (= dense, intermediate or
 347 open) and distance to the edge and their interaction effects on the mean offset of air and soil temperatures during summer and winter,
 348 and the evaporation. Dense forests were used as the reference management type. The effects for Tmin and Tmax can be found in the
 349 appendix (**Supplementary tables B1 and B2**). The coefficient estimates of the models are given and the significance of the effect is
 350 indicated with asterisks (* = $p < 0.05$, ** = $p < 0.01$, *** = $p < 0.001$).

<u>MEAN</u>	Summer air temperature offset (°C)	Summer soil temperature offset (°C)	Winter air temperature offset (°C)	Winter soil temperature offset (°C)	Evaporation (log- transformed, mm/year)
Mean annual macroclimate temperature (MAT) (°C)	-0.13	-1.57 ***	0.29 **	0.41 *	-
Intermediate forests	0.26	-	-	-	-
Open forests	0.60 *	-	-	-	-
Distance to the edge (log-transformed, m)	-0.08 *	-0.22 ***	-0.09 ***	-0.08 ***	-0.09 **
MAT × Distance	0.07 **	-	-	-	-
MAT × Intermediate	-	-	-	-	-
MAT × Open	-	-	-	-	-
Intermediate × Distance	-0.04	-	-	-	-
Open × Distance	-0.14 *	-	-	-	-

351

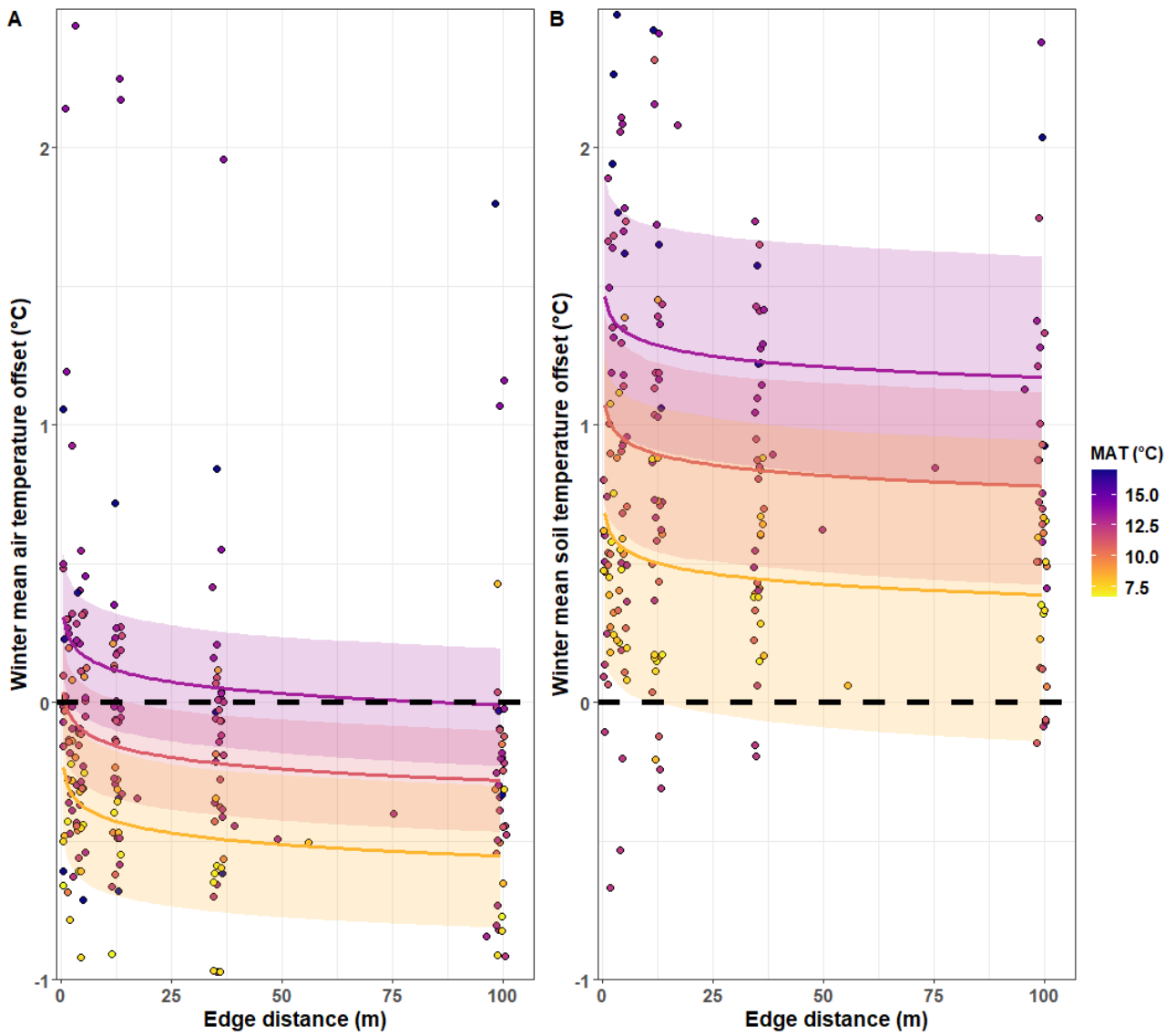
352 Interestingly, edge-to-interior gradients for the mean summer air offset were impacted by both
353 management as well as macroclimate (**Table 1, Figure 3A**). In summer, the mean air offset in open
354 forests was lower than in dense forests, but, as shown by the interaction between management type
355 and distance, dense forest edge zones showed a strong temperature offset directly at the edge and a
356 more gradual decrease in offset towards the interior (**Table 1, Figure 3A**). In open forests, on the
357 other hand, there was a steep decrease in offset between edge and interior. Edges in open forests were
358 thus subject to a reduced offset capacity and a stronger edge impact (**Figure 3A: effect of**
359 **management type × distance** shown in the different subpanels). Secondly, as demonstrated by the
360 significant interaction between the distance to the edge and MAT, the cooling of mean temperatures
361 in forest edge zones was more intense in warmer, southern regions but edge-to-interior gradients in
362 colder, northern regions were steeper and stabilized farther into the forest interior (**Figure 3A: effect**
363 **of MAT × distance** shown by the different colours). In sum, the strongest reduction of mean summer
364 sub-canopy temperatures could be found in dense forests located in warm regions, whereas in open
365 forests offsets were lower and the depth of edge influence was higher. We found that offsets up to
366 12.5 - 36.5 m from the edge were significantly different from the offset in the forest interior (99.5 m
367 from the edge) for the minimum summer air temperature and the mean and maximum air temperature
368 in winter (**Table 2**).

369



370

371 **Figure 3:** Predictions of the mean air temperature offset (°C, panel A) and soil temperature offset (°C, panel B) during the summer and
 372 the evaporation (mm per week, panel C) (mean and 95 % prediction intervals) as function of the distance to the edge (m). The different
 373 subpanels in A show the effect of the different management intensities. The lines show the model predictions of the significant
 374 interaction between edge distance and management, as well as between mean annual temperature (MAT, °C) and distance to the edge
 375 for the mean summer air temperature offset. The colours of the lines in panel A and B represent three distinct macroclimates (cold,
 376 intermediate and warm) within the studied macroclimate gradient. The dots in panel A and B represent the raw data points and their
 377 colour shows the mean annual macroclimate temperature outside the forest (MAT, °C); a small amount of jittering was added along
 378 the x-axis to improve clarity.



379

380 **Figure 4:** Predictions of the mean air temperature offset (°C, panel A) and soil temperature offset (°C, panel B) during the winter
 381 (mean and 95 % prediction intervals) as function of the distance to the edge (m). The colours of the lines represent three distinct
 382 macroclimates (cold, intermediate and warm) within the studied macroclimate gradient. The dots represent the raw data points and
 383 their colour shows the mean annual macroclimate temperature outside the forest (MAT, °C); a small amount of jittering was added
 384 along the x-axis to improve clarity.

385

386 **Table 2:** Depth of edge influence (m) (i.e. distance up to which the temperature offset was significantly different from the offset
 387 detected in the forest interior at 99.5 m from the edge) of the different temperature metrics (all in °C) during winter and summer.

Temperature metric		Depth of edge influence air temperature	Depth of edge influence soil temperature
In summer	Minimum temperature offset	Between 12.5 and 36.5 m	Between 1.5 and 4.5 m
	Mean temperature offset	Between 4.5 and 12.5 m	Between 1.5 and 4.5 m
	Maximum temperature offset	Between 1.5 and 4.5 m	Between 1.5 and 4.5 m
In winter	Minimum temperature offset	Between 1.5 and 4.5 m	No edge influence
	Mean temperature offset	Between 12.5 and 36.5 m	Between 1.5 and 4.5 m
	Maximum temperature offset	Between 12.5 and 36.5 m	Between 4.5 and 12.5 m

388

389 **Table 3:** The impact of local site characteristics (forest structure and composition, forest floor-biomass and soil texture) and regional
 390 landscape characteristics and macroclimate on the mean offset (°C) of air and soil temperatures during summer and winter, and the
 391 evaporation. The effects for Tmin and Tmax can be found in the appendix (**Supplementary table B3**). The direction of the effect is
 392 shown with arrows and the significance is indicated with asterisks (* = $p < 0.05$, ** = $p < 0.01$, *** = $p < 0.001$). MST = mean seasonal
 393 temperature. Explanatory variables without any significant effect were removed from the table.

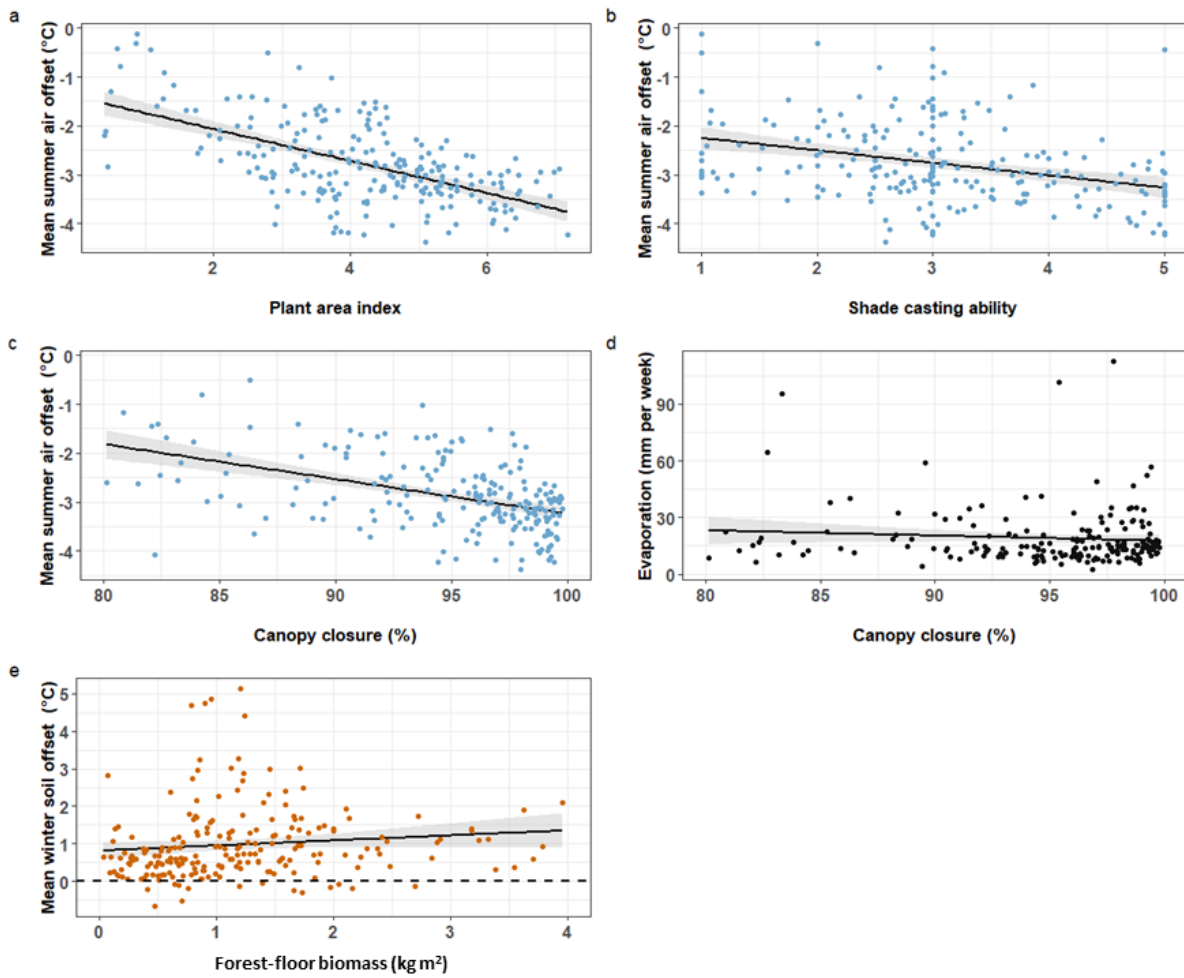
	Summer air temperature offset (°C)	Summer soil temperature offset (°C)	Winter air temperature offset (°C)	Winter soil temperature offset (°C)	Evaporation (log- transformed) (mm/year)
Plant area index (-)	↓***	↓***	↓***	↓***	-
Canopy height (m)	-	-	↓*	-	-
Shade casting ability (-)	↓**	-	-	-	↓*
Canopy closure (%)	↓***	↓*	↑**	-	↓***
Basal area (m²/ha)	-	-	-	-	↑***
Plant area index shrub layer (-)	-	-	-	↑***	-
Forest-floor biomass (kg/m²)	-	-	↑*	↑***	-
MST macroclimate outside forests (°C)	-	↓***	-	-	-
Northness (-)	-	-	↓**	-	-
Forest cover (%)	-	-	↓**	-	-

394

395 In a second set of models (**Table 3 and Supplementary table B3**), we studied the impact of regional
 396 and local site features on the offset and evaporation. During the summer, forest structural metrics
 397 were the main drivers of the cooling of mean and maximum temperatures in forest edge zones. In
 398 general, under canopies with a high plant area index and dense canopy closure there was a stronger,
 399 more negative, offset of mean and maximum temperatures in both air and soil (**Figure 5a and 5c**).
 400 Furthermore, the canopy species composition also controlled air temperature offsets, with an
 401 enhanced cooling (i.e. more negative offset) under trees with a high shade casting ability (**Figure 5b**).
 402 For soil summer temperatures, we also found a strong negative effect of the summer soil macroclimate
 403 on the mean and maximum soil temperature offsets in forests. The macroclimate was an important

404 driver of the minimum soil summer offset as well. Minimum air temperature offsets, on the other
405 hand were more positive in open forests and forests located in areas with warm summers, but
406 decreased in forests with a dense shrub layer. In short, mainly forest structure, and for soil
407 temperatures also the macroclimate, were important drivers of the summer offset. Likewise, forest
408 structure was an important regulator of the evaporation in forest edge zones. Evaporation was higher
409 in open forests (**Figure 5d**) dominated by trees with a low shade casting ability (**Table 3**).

410 The plant area index remained an important driver of the winter offsets, though the importance of the
411 different drivers shifted in this season (**Table 3 and Supplementary table B3**). Other drivers such
412 as slope, northness or canopy height were found to have a significant impact on the winter offset too.
413 Finally, also the forest-floor litter and humus biomass played a key role in the establishment of a
414 winter forest microclimate; a higher biomass in the humus and litter layer had an important positive
415 effect on the mean and maximum offsets in the soil (i.e. more positive offset, **Figure 5e**), and to a
416 lesser extent in the air during the winter.



417

418 **Figure 5:** Relationships between the offset and evaporation, and explanatory forest characteristics. Dots represent observations of the
 419 average air offset (°C) in summer in light blue, the evaporation (mm per week) in black or the average soil offset (°C) in winter in
 420 orange. Positive offset values indicate warmer temperatures in the forest whereas negative offsets represent cooler forest edge zones in
 421 comparison to free-air temperatures. The black lines show linear regressions with their 95% confidence intervals shaded in grey.

422 4. Discussion

423 4.1 Microclimatic changes across forest edges

424 Across Europe, we found that summer temperatures were generally more than 2°C cooler inside forest
425 edge zones. Maximum soil and air forest summer temperatures were on average cooler, whereas
426 minimum summer temperatures were warmer in comparison to free-air temperatures. Altogether,
427 forests were subject to a significant buffering (i.e. dampening of macroclimatic temperature variations
428 (De Frenne et al., 2021)), or thus fewer extreme temperatures and a lower temperature variability
429 during the summer (De Frenne et al., 2019; Zellweger et al., 2019). Moreover, we showed that
430 summer air and soil temperatures in the forest interior experienced a stronger buffering of mean and
431 warm ambient temperatures in comparison to forest edges. In addition to a cooling of warm
432 temperatures also evaporation was reduced in the interior. Increasingly cooler temperatures and a
433 higher humidity towards the forest interior are often observed patterns in forest patches which can be
434 attributed to a diminution of direct solar radiation and changes in wind conditions (Matlack, 1993;
435 Davies-Colley et al., 2000; Hylander, 2005; Schmidt et al., 2019). Indeed, temperature and humidity
436 are strongly correlated and can be linked with steep edge-oriented light gradients in forest edge zones
437 (Matlack, 1993; Chen et al., 1995; Davies-Colley et al., 2000; Kovács et al., 2017; Li et al., 2018). In
438 addition, since minimum summer temperatures were higher inside the forest and increased towards
439 the interior, also extreme summer temperatures were better buffered (i.e. macroclimatic fluctuations
440 were reduced) in the interior compared to edges in our study.

441 During winter, we found a negative impact of edge distance on the offsets as well. Mean and
442 maximum offsets dropped towards the interior, resulting in cooler forest interiors relative to open
443 areas and edges. However, directly at the edge and especially in the soil, winter offsets were mainly
444 positive. So, in winter, forest edge zones were often warmer than ambient air temperatures. Warmer
445 temperatures in forests during winter and night have been observed before (Chen et al., 1995;
446 Aussenac, 2000; Zellweger et al., 2019), but our results showed that this warming effect was mainly
447 apparent in forest soils and near the edge. In the soil, positive offsets in winter might be due to the
448 presence of an insulating layer of snow and/or litter (Bartlett, 2004; Graae et al., 2012; Fekete et al.,

449 2016). Deeper snow or thicker litter layers might build up near forest edges. Snow build up can result
450 from a higher canopy openness near the edge; or due to abrupt vegetation changes and the presence
451 of shrubs windblown snow and leaves might be trapped near edges and buffer soil temperatures
452 (Feeley, 2004; Vasconcelos and Luizão, 2004; Mellander et al., 2005; Myers-Smith et al., 2011).
453 Secondly, warming near the edge could also be due to heating of the soil, and subsequently via a heat-
454 flux the air above, due to more incoming solar radiation in leafless deciduous forests in winter and
455 via lateral penetration at the forest edge (Chen et al., 1995; Davies-Colley et al., 2000).

456 *Macroclimate: temperatures outside forests also influence offsets*
457 We found that the macroclimate interacted with edge distance: MAT positively affected the edge-to-
458 interior gradients in minimum, maximum and mean summer air temperature offset and, on the
459 contrary, had a negative impact on the maximum soil temperature offset during winter. For summer
460 air temperatures, the cooling of mean and maxima was strongest at the edge in warm regions but
461 differences diminished towards the interior as the slope in offset was steeper in cold regions.
462 Minimum summer air temperatures, on the other hand, were warmer in the interior and edge-to-
463 interior gradients stronger at more southern latitudes. Forests in warm, southern European regions
464 thus experienced the strongest reduction in temperature variability, especially in the forest interior. A
465 stronger buffering in warmer macroclimates is a worldwide phenomenon related to, among others,
466 seasonal effects, evapotranspiration and solar radiation inputs (De Frenne et al., 2019), showing that
467 forests could form temporary local microclimatic refugia under globally rising temperatures and
468 during heat waves. The main novelty here was the interaction with the distance to the forest edge and
469 that differences in offsets between regions were already present directly at the forest edge. In winter,
470 maximum soil temperatures were higher near the edge in warm regions whereas the edge-to-interior
471 gradients were almost absent in cooler regions. We therefore hypothesize that warmer soil
472 temperatures might be driven by heat accumulation in the soil near the edge, especially in warm
473 regions, or the buffering effect of a snow cover in northern areas (Chen et al., 1995; Davies-Colley et
474 al., 2000; Myers-Smith et al., 2011).

475 *Forest management*

476 Forest management also affected edge-to-interior patterns in the mean summer air offset (i.e. open
477 forests generated only a low temperature offset near the edge but were characterized by steeper
478 gradients in temperature). From the edge to interior, the offset in open forests increased from -2.1 to
479 -2.7°C. In dense forests nonetheless, temperatures were already strongly reduced at the edge with an
480 average offset of -2.8°C and reached mean values of -3.1°C in the interior. The average offset in
481 dense edges was similar to the average offset in open forest interiors. Dense forests were characterised
482 by a steep temperature drop at the edge, which can be caused by abrupt gradients in vegetation
483 structure between forest and adjacent land uses (Harper et al., 2005; Hofmeister et al., 2019). Dense
484 edge zones are, however, strong thermal insulators and establish smoother and weaker edge-to-
485 interior gradients, attributable to a higher complexity and a closed side-canopy protecting against
486 incoming radiation (Matlack, 1993; Aussenac, 2000; Kovács et al., 2017; Ehbrecht et al., 2019).
487 Steeper gradients, extending deeper towards the interior might manifest in intensively thinned forests
488 due to the lack of a side-canopy and higher openness.

489 *Impact of edge-to-interior gradients*

490 Edge influences in air temperature offsets were detected up to 12.5 m from the edge. Soil temperature
491 offsets were less sensitive to edge impact (significant differences up to only 4.5 m) and stabilized at
492 shorter distances as they are better buffered against temperature fluctuations, mainly depend on the
493 direct effect of soil heating and are less impacted by ambient conditions (i.e. air-mixing and transfer
494 of warm air from adjacent agricultural lands) (Chen et al., 1995; Davies-Colley et al., 2000; Li et al.,
495 2018). Edge influences were somewhat smaller but in accordance with previous studies suggesting
496 impacts up to approximately 40 - 50 m (Saunders et al., 1999; Davies-Colley et al., 2000; Schmidt et
497 al., 2019). We consider our estimates as rather conservative since, firstly, edge influences can vary
498 throughout the day and depend on weather conditions (Baker et al., 2014; Li et al., 2018). Second,
499 edge influences might also reach deeper into the forest although the effect is not significant or might
500 extend beyond the significant difference detected (i.e. lie somewhere between 12.5 and 36.5 m, our
501 next sample point). Third, it might be possible that microclimatic gradients are deeper than those

502 investigated in our set-up (i.e. more than 100 m); especially as our study design composes of southern
503 forest edges in the northern hemisphere which are known to have deeper edge influences than north-
504 oriented edges (Matlack, 1993; Chen et al., 1995; Hylander, 2005; Orczewska and Glista, 2005).

505

506 Considering an edge depth of 12.5 m and a total cumulative edge perimeter of roughly 9.4 billion m
507 for European deciduous forests (Meeussen et al., 2021), at least 11.7 million ha of broadleaved forest
508 in Europe are subject to edge influences in temperature. This is approximately 10% of the total area
509 of broadleaved forests of the European continent and the result of severe fragmentation and land-use
510 changes. As forests harbour the majority of terrestrial biodiversity (MEA, 2005), up to 80% of the
511 plant species richness in temperate forests is associated with the understorey (Gilliam, 2007), forest
512 fragmentation, apart from degradation and habitat loss, might form a threat to biodiversity. Our results
513 indicated that edge microclimates differ considerably from interior microclimates and therefore will
514 not support all organisms thriving in forest interiors. Due to their warm and open microclimate, edges
515 are often dominated by warmth-loving and light-demanding generalists and can harbour a lower
516 phylogenetic biodiversity than forest interiors (Honnay et al., 2002; Pellissier et al., 2013; Pfeifer et
517 al., 2017; Govaert et al., 2020; De Pauw et al., 2021). Nevertheless, edges themselves can be valuable
518 as well and management to maintain edges open might be important as they are biodiversity hotspots
519 and vital habitat types for certain species, in particular those that depend on half-open woody sites
520 and warmer microclimates (Duelli et al., 2002; De Smedt et al., 2019). Not only biodiversity will be
521 impacted by edge influences; spatial fluctuations in temperature will affect ecosystem functioning
522 and processes in edge zones such as litter decomposition or carbon drawdown (Riutta et al., 2012;
523 Fekete et al., 2016; Schmidt et al., 2019; Meeussen et al., 2021).

524 *4.2 Drivers of forest edge microclimates*

525 Canopy cover and composition are known as key drivers of sub-canopy temperatures (Matlack, 1993;
526 Aussenac, 2000; De Frenne et al., 2013; Frey et al., 2016; Zellweger et al., 2019). We showed that
527 vegetation structure and composition (i.e. shade casting ability) were important drivers of multiple

528 offset metrics in forest edge zones as well. In general, a higher plant area index and canopy closure
529 reduced both minimum and maximum air temperatures. Moreover, both explanatory variables might
530 also drive the stronger offset in forest interiors since both plant area index and canopy closure
531 increased from edge to interior (Meeussen et al., 2020). Forests with a high plant area index are
532 usually composed of a dense and multi-layered canopy with a high foliage biomass (Gower et al.,
533 1999; Kalácska et al., 2005). Dense canopies will intercept, absorb, reflect and emit radiation and
534 subsequently buffer both heating and cooling of understorey temperatures (Aussenac, 2000; Li et al.,
535 2018). Moreover, wind speed and patterns are altered under dense canopies, potentially causing an
536 even stronger offset between micro- and macroclimate (Aussenac, 2000; Renaud et al., 2011). A
537 complex and diverse stand structure, such as in old-growth forests or forests with a high diversity in
538 tree sizes and species, has therefore been advised for the creation of stable forest microclimates (Frey
539 et al., 2016; Kovács et al., 2017; Ehbrecht et al., 2019). Kovács et al. (2017) also suggested that,
540 besides an additional shading effect, vertical complexity would contribute to microclimatic buffering
541 by reducing the evaporation and increasing the humidity. We could, however, not find an impact of
542 plant area index, or thus foliage density on the evaporation. A high canopy closure and shade casting
543 ability did, however, reduce evaporation. This indicates that the penetration of direct radiation to the
544 forest floor via gaps in the canopy might be a stronger predictor of the integrated air humidity, besides
545 temperature, inside forests (Ehbrecht et al., 2019; Zellweger et al., 2019). Species composition further
546 affected the thermal buffering capacity of forests: we found that both mean and maximum summer
547 temperatures were lower in plots with more shade casting species (e.g. *Fagus sylvatica*) (Zellweger
548 et al., 2019).

549 During the winter months, forest structural metrics were still found to drive the offset, however, also
550 landscape characteristics and the forest-floor biomass were shown to play a vital role in regulating
551 forest temperatures (Greiser et al., 2018; Zellweger et al., 2019). The impact of forest structure on the
552 winter offset must be interpreted with caution as all structural metrics were determined during the
553 growing season and some of them (e.g. canopy openness) are subject to seasonal variation in

554 deciduous forests. However, even after leaf shedding, woody structural elements might still affect
555 sub-canopy temperatures via lateral shading or by affecting wind patterns near the edge (Bramer et
556 al., 2018; Greiser et al., 2018). On the other hand, our results supported the fact that this impact will
557 be less pronounced in winter than during the growing season and therefore microtopography and
558 other landscape characteristics can gain importance in regulating forest winter temperatures (Greiser
559 et al., 2018; Zellweger et al., 2019). Winter soil and air temperatures were higher in edge zones with
560 a thick forest-floor biomass. Changes in soil and forest floor colour will affect albedo and heat
561 accumulation (Bonan, 2008). A thick litter layer might also form a protecting layer on top of the soil,
562 moderating extreme temperatures and subsequently microbial processes and carbon, water and
563 nutrient fluxes (Ogée and Brunet, 2002; Fekete et al., 2016; Kovács et al., 2017; Meeussen et al.,
564 2021). During the winter, microtopography also affected the offset. Terrain features, besides
565 vegetation structure, are known to determine local temperatures and thus also winter forest
566 microclimates via, for instance, local variability in solar radiation, cold-air pooling in depressions or
567 wind exposure (Frey et al., 2016; Aalto et al., 2017; Bramer et al., 2018; Davis et al., 2019).

568 *4.3 Impacts and forest management guidelines*

569 We demonstrated that edge influences cannot be ignored in microclimate studies, and that edge
570 influences interacted with macroclimate and management. Our results further fill the knowledge gap
571 on how forest edges affect microclimatic buffering on a continental scale, improve microclimatic
572 mapping and contribute to future microclimatic analyses and the impact of global change on forest-
573 dwelling organisms; all key questions related to microclimate research (De Frenne et al., 2021).

574 Land-use change, in conjunction with forest degradation and fragmentation are increasing the
575 proportion of forest edges globally (Haddad et al., 2015; Riitters et al., 2016) and thus the impact of
576 the physical environment on forests. In combination with warming worldwide, the potential for forest
577 interiors to host and protect forest-dwelling organisms is threatened and therefore gaining importance
578 (De Frenne et al., 2013, 2019; Frey et al., 2016). To maintain interior microclimates and their
579 associated species, and to sustain short-term microclimatic refugia, fragmentation of large and old

580 forests should thus be avoided. Also, large-scale management practices, homogenizing forest stands
581 and creating interior edges and large canopy gaps, could better be replaced by small-scale cuts or
582 even single tree-selection systems (Frey et al., 2016; Hofmeister et al., 2019). Not only management
583 interventions might strongly increase sub-canopy temperatures but also disturbances such as
584 droughts, storms and insect outbreaks are predicted to increase in abundance and severity (Seidl et
585 al., 2017). Large-scale disturbances can damage forest canopies, reduce their insulating effect and
586 therefore threaten forest interior habitats and cause a shift in species composition (Stevens et al.,
587 2015). If cool and moist forest understories are desired to shelter forest interior specialists; smaller
588 forests, harbouring important species, could be protected by a buffer zone (i.e. an additional forested
589 edge area around the patch to maintain stable interior conditions in the forest patch) of at least 12.5
590 m deep, and via edge densification (i.e. creating a multi-layered edge with a low canopy openness
591 and high foliage density) (Matlack, 1993; Li et al., 2018). Finally, also planting species near the edge
592 which cast a deep shade on the forest floor (Zellweger et al., 2019) or aiming for a diverse mix of
593 shrubs and shade tolerant species forming gradual and dense side canopies in forest edges (Mourelle
594 et al., 2001; Niinemets, 2010; Jucker et al., 2015), might ameliorate microclimatic conditions and
595 buffer climate-change impacts in forests. To end, we note that there are many edge-related species
596 which do not prefer cool and humid forest microclimates. Highly-structured forest edge zones,
597 forming a gradual transition between forest and adjacent lands, are important habitats themselves for
598 many species (e.g., plants, butterflies, birds and insects) (Duelli et al., 2002; Lindgren et al., 2018).
599 Moreover, it should be kept in mind that also several typical forest herbs can benefit from temporary
600 higher light availability after natural disturbances and local gaps resulting from natural forest
601 succession or management interventions (Hilmers et al., 2018).

602 Acknowledgements

603 We thank Evy Ampoorter, Alicja Barć, Haben Blondeel, Filip and Kris Ceunen, Robbe De Beelde,
604 Emiel De Lombaerde, Bente J. Graae, Kent Hansson, Lionel Hertzog, Szymon Kuś, Dries Landuyt,
605 Iga Lewin, Pierre Lhoir, Sruthi M. Krishna Moorthy, Audrey Peiffer, Michael Perring, Mia Vedel
606 Sørensen, Matteo Tolosano, Sanne Van Den Berge and Lotte Van Nevel for providing support during
607 the fieldwork. Finally, we are grateful for the help of Luc Willems and Greet De bruyn for the
608 chemical analyses and Pieter Vermeir and Abdulwahhab Ghairi for the texture analysis.

609 Funding information

610 This work was supported by the European Research Council [ERC Starting Grant FORMICA no.
611 757833, 2018] (<http://www.formica.ugent.be>) and the FWO Scientific research network FLEUR
612 (www.fleur.ugent.be). Sanne Govaert was supported by the Research Foundation Flanders [FWO
613 project no. G0H1517N]. Thomas Vanneste received funding from the Special Research Fund (BOF)
614 from Ghent University [no. 01N02817]. Kim Calders was funded by the European Union's Horizon
615 2020 research and innovation programme under the Marie Skłodowska-Curie grant agreement [no.
616 835398]. Florian Zellweger received funding from the Swiss National Science Foundation [no.
617 193645].

618 References

- 619 Aalto, J., Riihimäki, H., Meineri, E., Hylander, K., Luoto, M., 2017. Revealing topoclimatic heterogeneity using
620 meteorological station data. *Int. J. Climatol.* 37, 544–556. <https://doi.org/10.1002/joc.5020>
- 621 Aussenac, G., 2000. Interactions between forest stands and microclimate: Ecophysiological aspects and consequences
622 for silviculture. *Ann. For. Sci.* <https://doi.org/10.1051/forest:2000119>
- 623 Baker, T.P., Jordan, G.J., Steel, E.A., Fountain-Jones, N.M., Wardlaw, T.J., Baker, S.C., 2014. Microclimate through
624 space and time: Microclimatic variation at the edge of regeneration forests over daily, yearly and decadal time
625 scales. *For. Ecol. Manage.* 334. <https://doi.org/10.1016/j.foreco.2014.09.008>
- 626 Bartlett, M.G., 2004. Snow and the ground temperature record of climate change. *J. Geophys. Res.* 109, F04008.
627 <https://doi.org/10.1029/2004JF000224>
- 628 Bates, D., Mächler, M., Bolker, B., Walker, S., 2015. Fitting linear mixed-effects models using lme4. *J. Stat. Softw.* 67,
629 1–48. <https://doi.org/10.18637/jss.v067.i01>
- 630 Bertrand, R., Lenoir, J., Piedallu, C., Riofrío-Dillon, G., de Ruffray, P., Vidal, C., Pierrat, J.-C., Gégout, J.-C., 2011.
631 Changes in plant community composition lag behind climate warming in lowland forests. *Nature* 479, 517–520.
632 <https://doi.org/10.1038/nature10548>
- 633 Bonan, G.B., 2008. Forests and climate change: Forcings, feedbacks, and the climate benefits of forests. *Science* (80-.).
634 <https://doi.org/10.1126/science.1155121>
- 635 Bramer, I., Anderson, B.J., Bennie, J., Bladon, A.J., De Frenne, P., Hemming, D., Hill, R.A., Kearney, M.R., Körner,
636 C., Korstjens, A.H., Lenoir, J., Maclean, I.M.D., Marsh, C.D., Morecroft, M.D., Ohlemüller, R., Slater, H.D.,
637 Suggitt, A.J., Zellweger, F., Gillingham, P.K., 2018. Advances in Monitoring and Modelling Climate at
638 Ecologically Relevant Scales, in: *Advances in Ecological Research*. Academic Press Inc., pp. 101–161.
639 <https://doi.org/10.1016/bs.aecr.2017.12.005>
- 640 Calders, K., Adams, J., Armston, J., Bartholomeus, H., Bauwens, S., Bentley, L.P., Chave, J., Danson, F.M., Demol,
641 M., Disney, M., Gaulton, R., Krishna Moorthy, S.M., Levick, S.R., Saarinen, N., Schaaf, C., Stovall, A., Terry,
642 L., Wilkes, P., Verbeeck, H., 2020. Terrestrial laser scanning in forest ecology: Expanding the horizon. *Remote
643 Sens. Environ.* <https://doi.org/10.1016/j.rse.2020.112102>
- 644 Chen, J., Franklin, J.F., Spies, T.A., 1995. Growing-season microclimatic gradients from clearcut edges into old-growth
645 Douglas-fir forests. *Ecol. Appl.* 5, 74–86. <https://doi.org/10.2307/1942053>
- 646 Chen, J., Saunders, S.C., Crow, T.R., Naiman, R.J., Brosofske, K.D., Mroz, G.D., Brookshire, B.L., Franklin, J.F.,
647 1999. Microclimate in forest ecosystem and landscape ecology. *Bioscience* 49, 288–297.
648 <https://doi.org/10.2307/1313612>
- 649 Chen, Y., Liu, Y., Zhang, J., Yang, W., He, R., Deng, C., 2018. Microclimate exerts greater control over litter

650 decomposition and enzyme activity than litter quality in an alpine forest-tundra ecotone. *Sci. Rep.* 8, 1–13.
651 <https://doi.org/10.1038/s41598-018-33186-4>

652 Davies-Colley, R.J., Payne, G.W., Van Elswijk, M., 2000. Microclimate gradients across a forest edge. *N. Z. J. Ecol.*
653 24, 111–121.

654 Davis, F.W., Synes, N.W., Fricker, G.A., McCullough, I.M., Serra-Diaz, J.M., Franklin, J., Flint, A.L., 2019. LiDAR-
655 derived topography and forest structure predict fine-scale variation in daily surface temperatures in oak savanna
656 and conifer forest landscapes. *Agric. For. Meteorol.* 269–270, 192–202.
657 <https://doi.org/10.1016/J.AGRFORMET.2019.02.015>

658 De Frenne, P., Lenoir, J., Luoto, M., Scheffers, B.R., Zellweger, F., Aalto, J., Ashcroft, M.B., Christiansen, D.M.,
659 Decocq, G., De Pauw, K., Govaert, S., Greiser, C., Gril, E., Hampe, A., Jucker, T., Klimes, D.H., Koelemeijer,
660 I.A., Lembrechts, J.J., Marrec, R., Meeussen, C., Ogée, J., Tyystjärvi, V., Vangansbeke, P., Hylander, K., 2021.
661 Forest microclimates and climate change: Importance, drivers and future research agenda. *Glob. Chang. Biol.*
662 *gcb.15569*. <https://doi.org/10.1111/gcb.15569>

663 De Frenne, P., Rodríguez-Sánchez, F., Coomes, D.A., Baeten, L., Verstraeten, G., Vellen, M., Bernhardt-Römermann,
664 M., Brown, C.D., Brunet, J., Cornelis, J., Decocq, G.M., Dierschke, H., Eriksson, O., Gilliam, F.S., Hédli, R.,
665 Heinken, T., Hermy, M., Hommel, P., Jenkins, M.A., Kelly, D.L., Kirby, K.J., Mitchell, F.J.G., Naaf, T.,
666 Newman, M., Peterken, G., Petřík, P., Schultz, J., Sonnier, G., Van Calster, H., Waller, D.M., Walther, G.R.,
667 White, P.S., Woods, K.D., Wulf, M., Graae, B.J., Verheyen, K., 2013. Microclimate moderates plant responses to
668 macroclimate warming. *Proc. Natl. Acad. Sci. U. S. A.* 110, 18561–18565.
669 <https://doi.org/10.1073/pnas.1311190110>

670 De Frenne, P., Rodríguez-Sánchez, F., De Schrijver, A., Coomes, D.A., Hermy, M., Vangansbeke, P., Verheyen, K.,
671 2015. Light accelerates plant responses to warming. *Nature plants*, 1(9), 1-3.
672 <https://doi.org/10.1038/NPLANTS.2015.110>

673 De Frenne, P., Zellweger, F., Rodríguez-Sánchez, F., Scheffers, B.R., Hylander, K., Luoto, M., Vellend, M., Verheyen,
674 K., Lenoir, J., 2019. Global buffering of temperatures under forest canopies. *Nat. Ecol. Evol.* 3, 744–749.
675 <https://doi.org/10.1038/s41559-019-0842-1>

676 De Pauw, K., Meeussen, C., Govaert, S., Sanczuk, P., Vanneste, T., Bernhardt-Römermann, M., Bollmann, K., Brunet,
677 J., Calders, K., Cousins, S., Diekmann, M., Hedwall, P., Iacopetti, G., Lenoir, J., Lindmo, S., Orczewska, A.,
678 Ponette, Q., Plue, J., Selvi, F., Spicher, F., Verbeeck, H., Vermeir, P., Zellweger, F., Verheyen, K., Vangansbeke,
679 P., De Frenne, P., 2021. Taxonomic, phylogenetic and functional diversity of understorey plants respond
680 differently to environmental conditions in European forest edges. *Journal of Ecology*.
681 <https://doi.org/10.1111/1365-2745.13671>

682 De Smedt, P., Baeten, L., Proesmans, W., Van de Poel, S., Van Keer, J., Giffard, B., Martin, L., Vanhulle, R., Brunet,
683 J., Cousins, S.A.O., Decocq, G., Deconchat, M., Diekmann, M., Gallet-Moron, E., Le Roux, V., Liira, J., Valdés,
684 A., Wulf, M., Andrieu, E., Hermy, M., Bonte, D., Verheyen, K., 2019. Strength of forest edge effects on litter-
685 dwelling macro-arthropods across Europe is influenced by forest age and edge properties. *Divers. Distrib.* 25,
686 963–974. <https://doi.org/10.1111/ddi.12909>

687 Duelli, P., Obrist, M. K., & Fluckiger, P. F., 2002. Forest edges are biodiversity hotspots—also for Neuroptera. *Acta*
688 *Zoologica Academiae Scientiarum Hungaricae*, 48(Suppl 2), 75-87.

689 Dutta, B., Grant, B.B., Congreves, K.A., Smith, W.N., Wagner-Riddle, C., VanderZaag, A.C., Tenuta, M., Desjardins,
690 R.L., 2018. Characterising effects of management practices, snow cover, and soil texture on soil temperature:
691 Model development in DNDC. *Biosyst. Eng.* 168, 54–72. <https://doi.org/10.1016/j.biosystemseng.2017.02.001>

692 Ehbrecht, M., Schall, P., Ammer, C., Fischer, M., Seidel, D., 2019. Effects of structural heterogeneity on the diurnal
693 temperature range in temperate forest ecosystems. *For. Ecol. Manage.* 432, 860–867.
694 <https://doi.org/10.1016/J.FORECO.2018.10.008>

695 EU-DEM. (2018). EU-digital elevation model (DEM). Version 1.1. Retrieved from <https://land.copernicus.eu/image>
696 [ery-in-situ/eu-dem/eu-dem-v1.1](https://land.copernicus.eu/image/ery-in-situ/eu-dem/eu-dem-v1.1)

697 Feeley, K.J., 2004. The effects of forest fragmentation and increased edge exposure on leaf litter accumulation. *J. Trop.*
698 *Ecol.* 20, 709–712. <https://doi.org/10.1017/S0266467404001828>

699 Fekete, I., Varga, C., Biró, B., Tóth, J.A., Várbíró, G., Lajtha, K., Szabó, G., Kotroczó, Z., 2016. The effects of litter
700 production and litter depth on soil microclimate in a central european deciduous forest. *Plant Soil* 398, 291–300.
701 <https://doi.org/10.1007/s11104-015-2664-5>

702 Frey, S.J.K., Hadley, A.S., Johnson, S.L., Schulze, M., Jones, J.A., Betts, M.G., 2016. Spatial models reveal the
703 microclimatic buffering capacity of old-growth forests. *Sci. Adv.* 2, e1501392.
704 <https://doi.org/10.1126/sciadv.1501392>

705 Geiger, R., Aron, R. H., Todhunter, P., 2009. *The climate near the ground.* Rowman & Littlefield.

706 Gilliam, F. S., 2007. The ecological significance of the herbaceous layer in temperate forest
707 ecosystems. *BioScience*, 57(10), 845-858. <https://doi.org/10.1641/B571007>

708 Govaert, S., Meeussen, C., Vanneste, T., Bollmann, K., Brunet, J., Cousins, S.A.O., Diekmann, M., Graae, B.J.,
709 Hedwall, P.-O., Heinken, T., Iacopetti, G., Lenoir, J., Lindmo, S., Orczewska, A., Perring, M.P., Ponette, Q.,
710 Plue, J., Selvi, F., Spicher, F., Tolosano, M., Vermeir, P., Zellweger, F., Verheyen, K., Vangansbeke, P., De
711 Frenne, P., 2020. Edge influence on understorey plant communities depends on forest management. *J. Veg. Sci.*
712 31. <https://doi.org/10.1111/jvs.12844>

713 Gower, S.T., Kucharik, C.J., Norman, J.M., 1999. Direct and indirect estimation of leaf area index, f(APAR), and net

714 primary production of terrestrial ecosystems. *Remote Sens. Environ.* 70, 29–51. <https://doi.org/10.1016/S0034->
715 4257(99)00056-5

716 Graae, B.J., De Frenne, P., Kolb, A., Brunet, J., Chabrierie, O., Verheyen, K., Pepin, N., Heinken, T., Zobel, M.,
717 Shevtsova, A., Nijs, I., Milbau, A., 2012. On the use of weather data in ecological studies along altitudinal and
718 latitudinal gradients. *Oikos* 121, 3–19. <https://doi.org/10.1111/j.1600-0706.2011.19694.x>

719 Greiser, C., Meineri, E., Luoto, M., Ehrlén, J., Hylander, K., 2018. Monthly microclimate models in a managed boreal
720 forest landscape. *Agric. For. Meteorol.* 250–251, 147–158. <https://doi.org/10.1016/J.AGRFORMET.2017.12.252>

721 Haddad, N.M., Brudvig, L.A., Clobert, J., Davies, K.F., Gonzalez, A., Holt, R.D., Lovejoy, T.E., Sexton, J.O., Austin,
722 M.P., Collins, C.D., Cook, W.M., Damschen, E.I., Ewers, R.M., Foster, B.L., Jenkins, C.N., King, A.J., Laurance,
723 W.F., Levey, D.J., Margules, C.R., Melbourne, B.A., Nicholls, A.O., Orrock, J.L., Song, D.-X., Townshend, J.R.,
724 2015. Habitat fragmentation and its lasting impact on Earth’s ecosystems. *Sci. Adv.* 1, e1500052.
725 <https://doi.org/10.1126/sciadv.1500052>

726 Hansen, M. C., Potapov, P. V., Moore, R., Hancher, M., Turubanova, S. A., Tyukavina, A., Thau, D., Stehman, S. V.,
727 Goetz S. J., Loveland, T. R., Kommareddy, A., Egorov, A., Chini, L., Justice, C. O., Townshend, J. R. G., 2013.
728 High-resolution global maps of 21st-century forest cover change. *Science*, 342(6160), 850–853. <https://doi.org/10.1126/science.1244693>

729

730 Harper, K.A., Macdonald, S.E., Burton, P.J., Chen, J., Broszofske, K.D., Saunders, S.C., Euskirchen, E.S., Roberts, D.,
731 Jaiteh, M.S., Esseen, P.-A., 2005. Edge influence on forest structure and composition in fragmented landscapes.
732 *Conserv. Biol.* 19, 768–782. <https://doi.org/10.1111/j.1523-1739.2005.00045.x>

733 Hilmers, T., Friess, N., Bäessler, C., Heurich, M., Brandl, R., Pretzsch, H., Seidl, R., Müller, J., 2018. Biodiversity along
734 temperate forest succession. *J. Appl. Ecol.* 55, 2756–2766. <https://doi.org/10.1111/1365-2664.13238>

735 Hofmeister, J., Hošek, J., Brabec, M., Střalková, R., Mýlová, P., Bouda, M., Pettit, J.L., Rydval, M., Svoboda, M.,
736 2019. Microclimate edge effect in small fragments of temperate forests in the context of climate change. *For.*
737 *Ecol. Manage.* 448, 48–56. <https://doi.org/10.1016/j.foreco.2019.05.069>

738 Honnay, O., Verheyen, K., Hermy, M., 2002. Permeability of ancient forest edges for weedy plant species invasion.
739 *For. Ecol. Manage.* 161, 109–122. [https://doi.org/10.1016/S0378-1127\(01\)00490-X](https://doi.org/10.1016/S0378-1127(01)00490-X)

740 Hothorn, T., Bretz, F., Westfall, P., 2008. Simultaneous inference in general parametric models. *Biometrical J.*
741 <https://doi.org/10.1002/bimj.200810425>

742 Hylander, K., 2005. Aspect modifies the magnitude of edge effects on bryophyte growth in boreal forests. *J. Appl. Ecol.*
743 42, 518–525. <https://doi.org/10.1111/j.1365-2664.2005.01033.x>

744 International Civil Aviation Organization, 1993. Manual of the ICAO standard atmosphere: extended to 80 kilometres
745 (262 500 feet), 3rd ed. International Civil Aviation Organization, Montreal, Quebec.

746 IPCC, 2018. Summary for Policymakers. In: Global Warming of 1.5°C. An IPCC Special Report on the impacts of
747 global warming of 1.5°C above pre-industrial levels and related global greenhouse gas emission pathways, in the
748 context of strengthening the global response to the threat of climate change, sustainable development, and efforts
749 to eradicate poverty [Masson-Delmotte, V., P. Zhai, H.-O. Pörtner, D. Roberts, J. Skea, P.R. Shukla, A. Pirani, W.
750 Moufouma-Okia, C. Péan, R. Pidcock, S. Connors, J.B.R. Matthews, Y. Chen, X. Zhou, M.I. Gomis, E. Lonnoy,
751 T. Maycock, M. Tignor, and T. Waterfield (eds.)]. World Meteorological Organization, Geneva, Switzerland, 32
752 pp.

753 ISO 11277, 2009. Soil quality – Determination of particle size distribution in mineral soil material – Method by sieving
754 and sedimentation ISO, Geneva.

755 Jucker, T., Bouriaud, O., Coomes, D.A., 2015. Crown plasticity enables trees to optimize canopy packing in mixed-
756 species forests. *Funct. Ecol.* 29, 1078–1086. <https://doi.org/10.1111/1365-2435.12428>

757 Kalácska, M., Calvo-Alvarado, J.C., Sánchez-Azofeifa, G.A., 2005. Calibration and assessment of seasonal changes in
758 leaf area index of a tropical dry forest in different stages of succession. *Tree Physiol.* 25, 733–744.
759 <https://doi.org/10.1093/TREEPHYS/25.6.733>

760 Karger, D.N., Conrad, O., Böhner, J., Kawohl, T., Kreft, H., Soria-Auza, R.W., Zimmermann, N.E., Linder, H.P.,
761 Kessler, M., 2017. Climatologies at high resolution for the earth’s land surface areas. *Sci. Data* 4, 170122.
762 <https://doi.org/10.1038/sdata.2017.122>

763 Kovács, B., Tinya, F., Ódor, P., 2017. Stand structural drivers of microclimate in mature temperate mixed forests.
764 *Agric. For. Meteorol.* 234–235, 11–21. <https://doi.org/10.1016/j.agrformet.2016.11.268>

765 Kuznetsova, A., Brockhoff, P.B., Christensen, R.H.B., 2017. lmerTest package: tests in linear mixed effects models. *J.*
766 *Stat. Softw.* 82, 1–26. <https://doi.org/10.18637/jss.v082.i13>

767 Lembrechts, J.J., Lenoir, J., 2019. Microclimatic conditions anywhere at any time! *Glob. Chang. Biol.*
768 <https://doi.org/10.1111/gcb.14942>

769 Li, Y., Kang, W., Han, Y., Song, Y., 2018. Spatial and temporal patterns of microclimates at an urban forest edge and
770 their management implications. *Environ. Monit. Assess.* 190, 93. <https://doi.org/10.1007/s10661-017-6430-4>

771 Lindgren, J., Kimberley, A., Cousins, S.A.O., 2018. The complexity of forest borders determines the understorey
772 vegetation. *Appl. Veg. Sci.* 21, 85–93. <https://doi.org/10.1111/avsc.12344>

773 Magura, T., 2002. Carabids and forest edge: spatial pattern and edge effect. *For. Ecol. Manage.* 157, 23–37.
774 [https://doi.org/10.1016/S0378-1127\(00\)00654-X](https://doi.org/10.1016/S0378-1127(00)00654-X)

775 Matlack, G.R., 1993. Microenvironment variation within and among forest edge sites in the eastern United States. *Biol.*
776 *Conserv.* 66, 185–194. [https://doi.org/10.1016/0006-3207\(93\)90004-K](https://doi.org/10.1016/0006-3207(93)90004-K)

777 MEA., 2005. Millennium Ecosystem Assessment. Ecosystems and human well-being: Biodiversity synthesis.

778 Washington, DC: Millennium Ecosystem Assessment

779 Meeussen, C., Govaert, S., Vanneste, T., Calders, K., Bollmann, K., Brunet, J., Cousins, S.A.O., Diekmann, M., Graae,
780 B.J., Hedwall, P.O., Krishna Moorthy, S.M., Iacopetti, G., Lenoir, J., Lindmo, S., Orczewska, A., Ponette, Q.,
781 Plue, J., Selvi, F., Spicher, F., Tolosano, M., Verbeeck, H., Verheyen, K., Vangansbeke, P., De Frenne, P., 2020.
782 Structural variation of forest edges across Europe. *For. Ecol. Manage.* 462, 117929.
783 <https://doi.org/10.1016/j.foreco.2020.117929>

784 Meeussen, C., Govaert, S., Vanneste, T., Haesen, S., Van Meerbeek, K., Bollmann, K., Brunet, J., Calders, K., Cousins,
785 S.A.O., Diekmann, M., Graae, B.J., Iacopetti, G., Lenoir, J., Orczewska, A., Ponette, Q., Plue, J., Selvi, F.,
786 Spicher, F., Sørensen, M.V., Verbeeck, H., Vermeir, P., Verheyen, K., Vangansbeke, P., De Frenne, P., 2021.
787 Drivers of carbon stocks in forest edges across Europe. *Sci. Total Environ.* 759, 143497.
788 <https://doi.org/10.1016/j.scitotenv.2020.143497>

789 Mellander, P.E., Laudon, H., Bishop, K., 2005. Modelling variability of snow depths and soil temperatures in Scots pine
790 stands, in: *Agricultural and Forest Meteorology*. Elsevier, pp. 109–118.
791 <https://doi.org/10.1016/j.agrformet.2005.08.008>

792 Mourelle, C., Kellman, M., Kwon, L., 2001. Light occlusion at forest edges: an analysis of tree architectural
793 characteristics. *For. Ecol. Manage.* 154, 179–192. [https://doi.org/10.1016/S0378-1127\(00\)00624-1](https://doi.org/10.1016/S0378-1127(00)00624-1)

794 Muñoz Sabater, J., 2019. ERA5-Land hourly data from 1981 to present. Copernicus Climate Change Service (C3S)
795 Climate Data Store (CDS). (Accessed on 23-02-2021), <https://doi.org/10.24381/cds.e2161bac>

796 Murcia, C., 1995. Edge effects in fragmented forests: implications for conservation. *Trends Ecol. Evol.* 10, 58–62.
797 [https://doi.org/10.1016/S0169-5347\(00\)88977-6](https://doi.org/10.1016/S0169-5347(00)88977-6)

798 Myers-Smith, I. H., Forbes, B. C., Wilmking, M., Hallinger, M., Lantz, T., Blok, D., Tape, K. D., Macias-Fauria, M.,
799 Sass-Klaassen, U., Lévesque, E., Boudrea, S., Ropars, P., Hermanutz, L., Trant, A., Siegwart Collier, L., Weijers,
800 S., Rozema, J., Rayback, S. A., Schmidt, N. M., Schaepman-Strub, G., Wipf, S., Rixen, C., Ménard, C. B., Venn,
801 S., Goetz, S., Andreu-Hayles, L., Elmendorf, S., Ravolainen, V., Welker, J., Grogan, P., Epstein, H. E., Hik, D.
802 S., 2011. Shrub expansion in tundra ecosystems: dynamics, impacts and research priorities. *Environmental*
803 *Research Letters*, 6(4), 045509.

804 Niinemets, Ü., 2010. A review of light interception in plant stands from leaf to canopy in different plant functional
805 types and in species with varying shade tolerance. *Ecol. Res.* 25, 693–714. [https://doi.org/10.1007/s11284-010-](https://doi.org/10.1007/s11284-010-0712-4)
806 [0712-4](https://doi.org/10.1007/s11284-010-0712-4)

807 Ogée, J., Brunet, Y., 2002. A forest floor model for heat and moisture including a litter layer. *J. Hydrol.* 255, 212–233.
808 [https://doi.org/10.1016/S0022-1694\(01\)00515-7](https://doi.org/10.1016/S0022-1694(01)00515-7)

809 Orczewska, A., Glista, A., 2005. Floristic analysis of the two woodland-meadow ecotones differing in orientation of the

810 forest edge. *Polish J. Ecol.* 53, 365–382.

811 Papaioannou, G., Vouraki, K., Kerkides, P., 1996. Piche evaporimeter data as a substitute for Penman equation's
812 aerodynamic term. *Agric. For. Meteorol.* 82, 83–92.

813 Paul, K.I., Polglase, P.J., Smethurst, P.J., O'Connell, A.M., Carlyle, C.J., Khanna, P.K., 2004. Soil temperature under
814 forests: A simple model for predicting soil temperature under a range of forest types. *Agric. For. Meteorol.* 121,
815 167–182. <https://doi.org/10.1016/j.agrformet.2003.08.030>

816 Pellissier, V., Bergès, L., Nedeltcheva, T., Schmitt, M.-C., Avon, C., Cluzeau, C., Dupouey, J.-L., 2013. Understorey
817 plant species show long-range spatial patterns in forest patches according to distance-to-edge. *J. Veg. Sci.* 24, 9–
818 24. <https://doi.org/10.1111/j.1654-1103.2012.01435.x>

819 Pfeifer, M., Lefebvre, V., Peres, C.A., Banks-Leite, C., Wearn, O.R., Marsh, C.J., Butchart, S.H.M., Arroyo-Rodríguez,
820 V., Barlow, J., Cerezo, A., Cisneros, L., D'Cruze, N., Faria, D., Hadley, A., Harris, S.M., Klingbeil, B.T.,
821 Kormann, U., Lens, L., Medina-Rangel, G.F., Morante-Filho, J.C., Olivier, P., Peters, S.L., Pidgeon, A., Ribeiro,
822 D.B., Scherber, C., Schneider-Maunoury, L., Struebig, M., Urbina-Cardona, N., Watling, J.I., Willig, M.R.,
823 Wood, E.M., Ewers, R.M., 2017. Creation of forest edges has a global impact on forest vertebrates. *Nature* 551,
824 187–191. <https://doi.org/10.1038/nature24457>

825 R Core Team, 2020. R: A language and environment for statistical computing. R Foundation for Statistical Computing.
826 Austria. URL, Vienna <https://www.R-project.org/>.

827 Remy, E., Wuyts, K., Boeckx, P., Ginzburg, S., Gundersen, P., Demey, A., Van Den Bulcke, J., Van Acker, J.,
828 Verheyen, K., 2016. Strong gradients in nitrogen and carbon stocks at temperate forest edges. *For. Ecol. Manage.*
829 376, 45–58. <https://doi.org/10.1016/j.foreco.2016.05.040>

830 Renaud, V., Innes, J.L., Dobbertin, M., Rebetez, M., 2011. Comparison between open-site and below-canopy climatic
831 conditions in Switzerland for different types of forests over 10 years (1998-2007). *Theor. Appl. Climatol.* 105,
832 119–127. <https://doi.org/10.1007/s00704-010-0361-0>

833 Ries, L., Fletcher, R.J., Battin, J., Sisk, T.D., 2004. Ecological Responses to Habitat Edges: Mechanisms, Models, and
834 Variability Explained. *Annu. Rev. Ecol. Evol. Syst.* 35, 491–522.
835 <https://doi.org/10.1146/annurev.ecolsys.35.112202.130148>

836 Riitters, K., Wickham, J., Costanza, J.K., Vogt, P., 2016. A global evaluation of forest interior area dynamics using tree
837 cover data from 2000 to 2012. *Landsc. Ecol.* 31, 137–148. <https://doi.org/10.1007/s10980-015-0270-9>

838 Riutta, T., Slade, E.M., Bebbler, D.P., Taylor, M.E., Malhi, Y., Riordan, P., Macdonald, D.W., Morecroft, M.D., 2012.
839 Experimental evidence for the interacting effects of forest edge, moisture and soil macrofauna on leaf litter
840 decomposition. *Soil Biol. Biochem.* 49, 124–131. <https://doi.org/10.1016/j.soilbio.2012.02.028>

841 Sanczuk, P., Govaert, S., Meeussen, C., De Pauw, K., Vanneste, T., Depauw, L., Moreira, X., Schoelynck, J., De

842 Boevre, M., De Saeger, S., Bollmann, K., Brunet, J., Cousins, S. A. O., Plue, J., Diekmann, M., Graae, B.
843 J., Hedwall, P., Iacopetti, G., Lenoir, J., Orczewska, A., Ponette, Q., Selvi, F., Spicher, F., Vermeir, P., Calders,
844 K., Verbeeck, H., Verheyen, K., Vangansbeke, P., De Frenne, P., 2021. Small scale environmental variation
845 modulates plant defence syndromes of understorey plants in deciduous forests of Europe. *Global Ecology and*
846 *Biogeography*, 30(1), 205-219. <https://doi.org/10.1111/geb.13216>

847 Saunders, S.C., Chen, J., Drummer, T.D., Crow, T.R., 1999. Modeling temperature gradients across edges over time in
848 a managed landscape. *For. Ecol. Manage.* 117, 17–31. [https://doi.org/10.1016/S0378-1127\(98\)00468-X](https://doi.org/10.1016/S0378-1127(98)00468-X)

849 Schmidt, M., Jochheim, H., Kersebaum, K.-C., Lischeid, G., Nendel, C., 2017. Gradients of microclimate, carbon and
850 nitrogen in transition zones of fragmented landscapes – a review. *Agric. For. Meteorol.* 232, 659–671.
851 <https://doi.org/10.1016/J.AGRFORMET.2016.10.022>

852 Schmidt, M., Lischeid, G., Nendel, C., 2019. Microclimate and matter dynamics in transition zones of forest to arable
853 land. *Agric. For. Meteorol.* 268, 1–10. <https://doi.org/10.1016/j.agrformet.2019.01.001>

854 Seidl, R., Thom, D., Kautz, M., Martin-Benito, D., Peltoniemi, M., Vacchiano, G., Wild, J., Ascoli, D., Petr, M.,
855 Honkaniemi, J., Lexer, M.J., Trotsiuk, V., Mairota, P., Svoboda, M., Fabrika, M., Nagel, T.A., Reyer, C.P.O.,
856 2017. Forest disturbances under climate change. *Nat. Clim. Chang.* <https://doi.org/10.1038/nclimate3303>

857 Stevens, J.T., Safford, H.D., Harrison, S., Latimer, A.M., 2015. Forest disturbance accelerates thermophilization of
858 understory plant communities. *J. Ecol.* 103, 1253–1263. <https://doi.org/10.1111/1365-2745.12426>

859 Vasconcelos, H.L., Luizão, F.J., 2004. Litter production and litter nutrient concentrations in a fragmented amazonian
860 landscape. *Ecol. Appl.* 14, 884–892. <https://doi.org/10.1890/03-5093>

861 Verheyen, K., Baeten, L., De Frenne, P., Bernhardt-Römermann, M., Brunet, J., Cornelis, J., Decocq, G., Dierschke, H.,
862 Eriksson, O., Hédl, R., Heinken, T., Hermy, M., Hommel, P., Kirby, K., Naaf, T., Peterken, G., Petřík, P.,
863 Pfadenhauer, J., Van Calster, H., Walther, G.R., Wulf, M., Verstraeten, G., 2012. Driving factors behind the
864 eutrophication signal in understorey plant communities of deciduous temperate forests. *J. Ecol.* 100, 352–365.
865 <https://doi.org/10.1111/j.1365-2745.2011.01928.x>

866 Young, A., Mitchell, N., 1994. Microclimate and vegetation edge effects in a fragmented podocarp-broadleaf forest in
867 New Zealand. *Biol. Conserv.* 67, 63–72. [https://doi.org/10.1016/0006-3207\(94\)90010-8](https://doi.org/10.1016/0006-3207(94)90010-8)

868 Zellweger, F., Coomes, D., Lenoir, J., Depauw, L., Maes, S.L., Wulf, M., Kirby, K.J., Brunet, J., Kopecký, M., Máliš,
869 F., Schmidt, W., Heinrichs, S., den Ouden, J., Jaroszewicz, B., Buyse, G., Spicher, F., Verheyen, K., De Frenne,
870 P., 2019. Seasonal drivers of understorey temperature buffering in temperate deciduous forests across Europe.
871 *Glob. Ecol. Biogeogr.* 28, 1774–1786. <https://doi.org/10.1111/geb.12991>

872 Zellweger, F., de Frenne, P., Lenoir, J., Vangansbeke, P., Verheyen, K., Bernhardt-Römermann, M., Baeten, L., Hédl,
873 R., Berki, I., Brunet, J., van Calster, H., Chudomelová, M., Decocq, G., Dirnböck, T., Durak, T., Heinken, T.,

874 Jaroszewicz, B., Kopecký, M., Máliš, F., Macek, M., Malicki, M., Naaf, T., Nagel, T.A., Ortmann-Ajkai, A.,
875 Petřík, P., Pielech, R., Reczynska, K., Schmidt, W., Standovár, T., Swierkosz, K., Teleki, B., Vild, O., Wulf, M.,
876 Coomes, D., 2020. Forest microclimate dynamics drive plant responses to warming. *Science* (80-.). 368.
877 <https://doi.org/10.1126/science.aba6880>
878 Zuur, A., Ieno, E., Walker, N., Saveliev, A., Smith, G., 2009. Mixed effects modelling for nested data, in: Zuur, A.F.,
879 Ieno, E.N., Walker, N.J., Saveliev, A.A., Smith, G.M. (Eds.), *Mixed Effects Models and Extensions in Ecology*
880 with R. Springer, New York, NY, USA, pp. 101–142.

881 **Supplementary information: Microclimatic**
882 **edge-to-interior gradients of European**
883 **deciduous forests**

884 Appendix A: Additional information material and method section



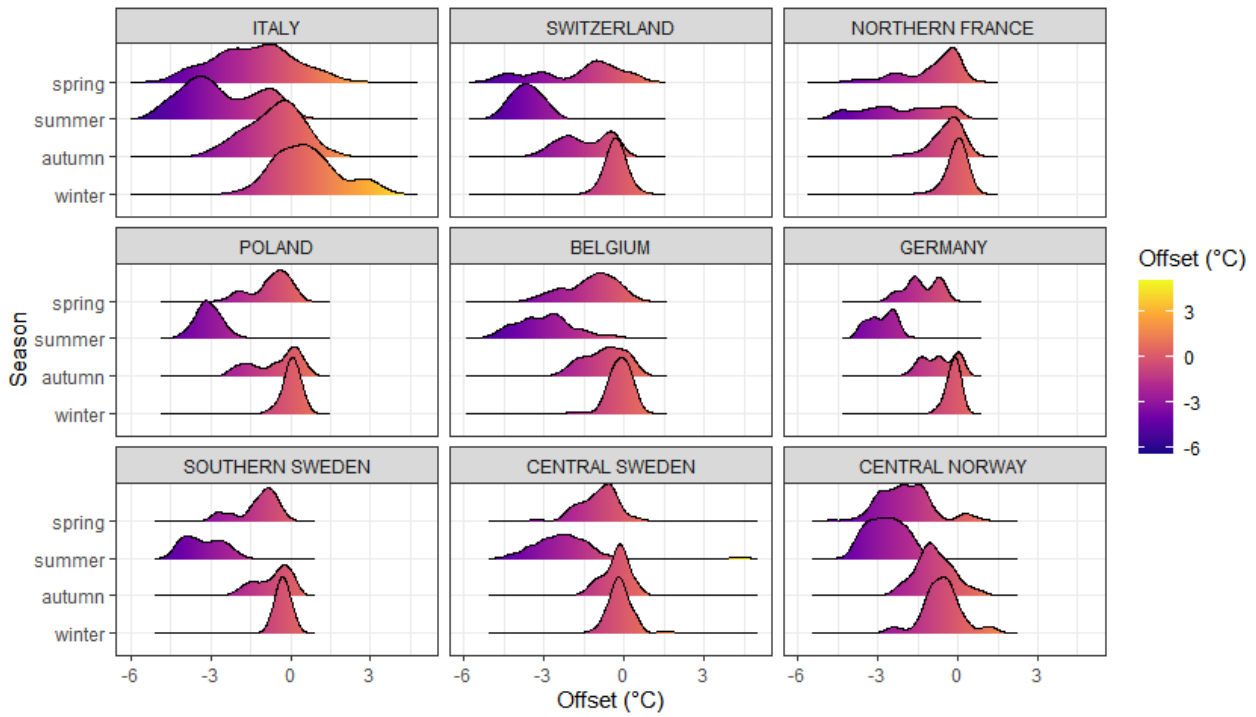
885
886 **Figure A1:** Set-up of the temperature sensors. Left: pole with radiation sheet, covering the air temperature data logger. Right: soil
887 logger protected by a plastic tube (here at the surface, normally buried at a depth of 5 cm).

888 **Table A1:** Shade casting ability scores for the tree and shrub species present in the dataset (one denotes a very low shade casting ability,
 889 whereas five reflects the opposite). The shade casting ability scores were adapted from Verheyen et al. (2012) and Govaert et al. (2020).

Species	Shade casting ability		
<i>Acer campestre</i>	3	<i>Ligustrum vulgare</i>	3
<i>Acer monspessulanum</i>	4	<i>Malus sylvestris</i>	2
<i>Acer opalus</i>	4	<i>Ostrya carpinifolia</i>	4
<i>Acer platanoides</i>	4	<i>Phillyrea latifolia</i>	3
<i>Acer pseudoplatanus</i>	4	<i>Picea abies</i>	4
<i>Aesculus hippocastanum</i>	4	<i>Pinus sylvestris</i>	1
<i>Alnus glutinosa</i>	3	<i>Populus canadensis</i>	2
<i>Alnus incana</i>	3	<i>Populus tremula</i>	2
<i>Arbutus unedo</i>	3	<i>Prunus avium</i>	3
<i>Betula pendula</i>	1	<i>Prunus padus</i>	3
<i>Betula pubescens</i>	1	<i>Prunus serotina</i>	3
<i>Carpinus betulus</i>	5	<i>Prunus spinosa</i>	3
<i>Castanea sativa</i>	3	<i>Pyrus communis</i> subsp. <i>pyraster</i>	2
<i>Cornus mas</i>	2	<i>Quercus cerris</i>	3
<i>Cornus sanguinea</i>	2	<i>Quercus ilex</i>	4
<i>Corylus avellana</i>	3	<i>Quercus petraea</i>	3
<i>Crataegus laevigata</i>	3	<i>Quercus pubescens</i>	3
<i>Crataegus monogyna</i>	3	<i>Quercus robur</i>	2
<i>Cytisus scoparius</i>	2	<i>Quercus rubra</i>	3
<i>Erica arborea</i>	2	<i>Salix caprea</i>	2
<i>Erica scoparia</i>	2	<i>Salix spec.</i>	2
<i>Fagus sylvatica</i>	5	<i>Sambucus nigra</i>	3
<i>Frangula alnus</i>	3	<i>Sorbus aucuparia</i>	2
<i>Fraxinus excelsior</i>	3	<i>Sorbus domestica</i>	2
<i>Fraxinus ornus</i>	3	<i>Sorbus torminalis</i>	2
<i>Ilex aquifolium</i>	5	<i>Tilia cordata</i>	4
<i>Juglans regia</i>	3	<i>Ulmus glabra</i>	4
<i>Juniperus communis</i>	2	<i>Ulmus minor</i>	3
		<i>Viburnum opulus</i>	3

890

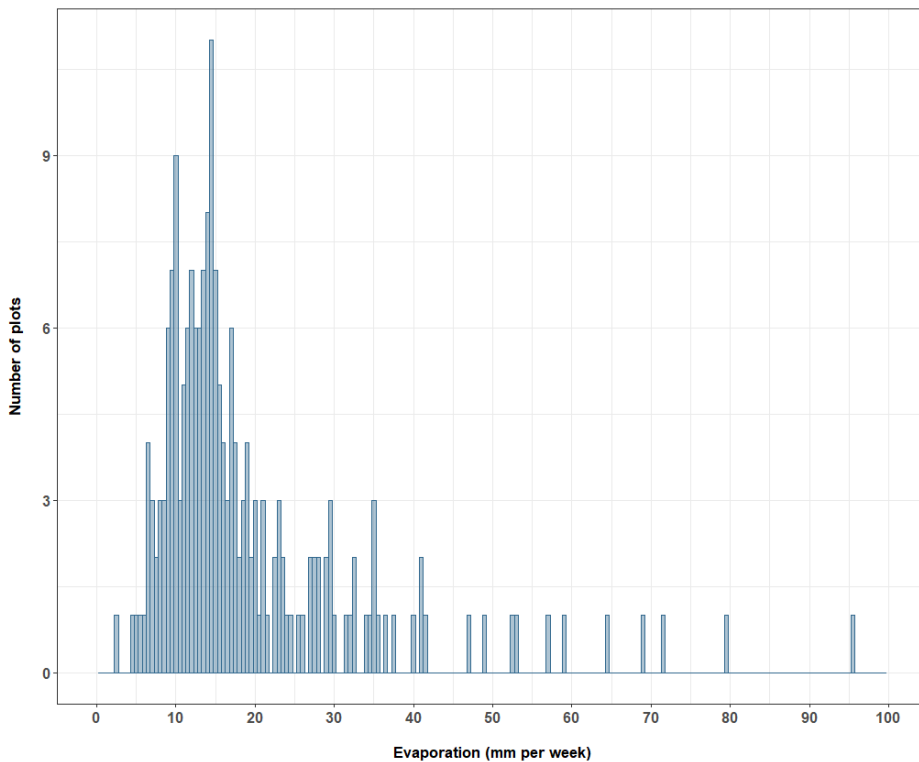
891



893

894 **Figure B1:** Overview of the mean monthly air temperature offsets (°C) per season in the nine different regions, shown in the subpanels

895 from southern (upper left corner) to more northern regions (bottom right corner).



906 **Figure B2:** Overview of the variation in evaporation across all plots (n = 201).

907 **Table B1:** Overview of the results of the linear mixed-effect models using the design variables (mean annual temperature (= MAT,
908 from the reference sensors), forest management type and distance to the edge and their interaction effects on the maximum offset of
909 air and soil temperatures during summer and winter. Dense forests were used as the reference management type. The coefficient
910 estimates of the models are given and the significance of the effect is indicated with asterisks (* = $p < 0.05$, ** = $p < 0.01$, *** = $p <$
911 0.001).

<u>MAXIMUM</u>	Summer air temperature offset (°C)	Summer soil temperature offset (°C)	Winter air temperature offset (°C)	Winter soil temperature offset (°C)
Mean annual macroclimate temperature (MAT) (°C)	-0.42	-1.45 *	-	0.36
Intermediate forests	-	-	-	-
Open forests	-	-	-	-
Distance to the edge (log-transformed, m)	-0.64 ***	-0.41 ***	-0.57 ***	-0.14 ***
MAT × Distance	0.31 *	-	-	-0.06 *
MAT × Intermediate	-	-	-	-
MAT × Open	-	-	-	-
Intermediate × Distance	-	-	-	-
Open × Distance	-	-	-	-

912

913 **Table B2:** Overview of the results of the linear mixed-effect models using the design variables (mean annual temperature (= MAT,
914 from the reference sensors), forest management type and distance to the edge and their interaction effects on the minimum offset of air
915 and soil temperatures during summer and winter. Dense forests were used as the reference management type. The coefficient estimates
916 of the models are given and the significance of the effect is indicated with asterisks (* = $p < 0.05$, ** = $p < 0.01$, *** = $p < 0.001$).

<u>MINIMUM</u>	Summer air temperature offset (°C)	Summer soil temperature offset (°C)	Winter air temperature offset (°C)	Winter soil temperature offset (°C)
Mean annual macroclimate temperature (MAT) (°C)	0.02	-	0.41 *	0.55 ***
Intermediate forests	-	-	-	-
Open forests	-	-	-	-
Distance to the edge (log-transformed, m)	0.11 ***	-0.1 ***	0.06 ***	-
MAT × Distance	0.05 **	-	-	-
MAT × Intermediate	-	-	-	-
MAT × Open	-	-	-	-
Intermediate × Distance	-	-	-	-
Open × Distance	-	-	-	-

917

918 **Table B3:** The impact of local site features (forest structure and composition, the forest-floor biomass and soil texture) and regional
 919 landscape characteristics and macroclimate on the Tmax (average maximum temperature offset, °C) and Tmin (average minimum
 920 temperature offset, °C) of the air and soil temperature during summer and winter. The direction of the effect is shown with arrows,
 921 whereas the significance is indicated with asterisks (* = $p < 0.05$, ** = $p < 0.01$, *** = $p < 0.001$). MST = mean seasonal temperature.
 922 Explanatory variables without any significant effect were removed from the table.

	Summer air temperature offset (°C)		Summer soil temperature offset (°C)		Winter air temperature offset (°C)		Winter soil temperature offset (°C)	
	Tmax	Tmin	Tmax	Tmin	Tmax	Tmin	Tmax	Tmin
Plant area index (-)	↓***	↑***	↓***	↓***	↓***	↑***	↓***	↓*
Canopy height (m)	-	-	-	-	-	↓**	↓**	-
Shade casting ability (-)	↓*	-	-	-	-	-	↑*	-
Canopy closure (%)	↓***	↑***	↓*	-	-	-	-	-
Plant area index shrub layer (-)	-	↓***	-	-	-	↓**	↑*	↑***
Forest-floor biomass (kg/m²)	-	-	-	-	↑*	-	↑***	↑***
Distance to coast (km)	-	-	-	-	↓*	-	-	-
MST macroclimate outside forests (°C)	-	↑*	↓***	↓***	-	↑*	↑.	-
Slope (°)	-	-	-	-	↓***	↑***	↑**	-
Northness (-)	-	↑*	-	-	↓***	-	↓*	-
Forest cover (%)	-	-	-	↓*	-	-	-	-

923

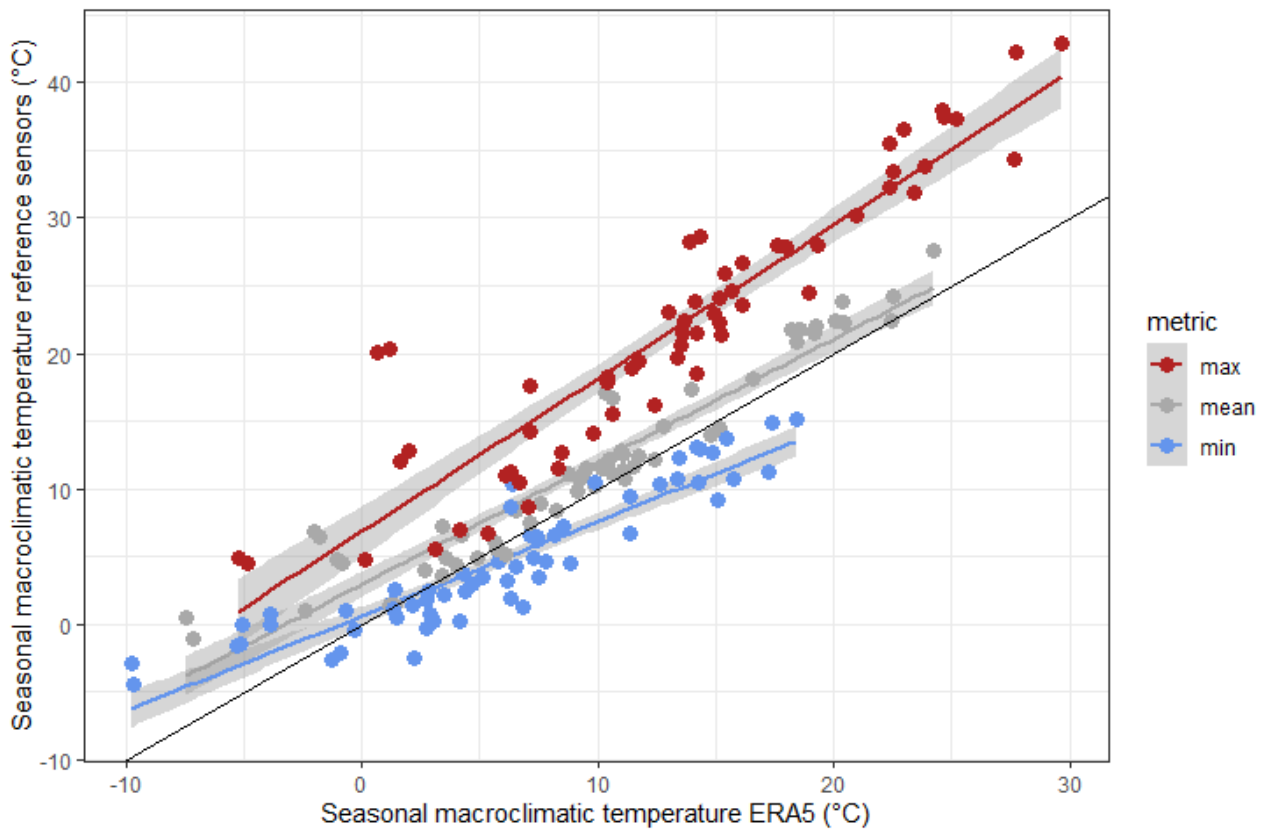
924 Appendix C: Comparison of macroclimatic data obtained from our reference sensors
925 placed outside the forests with gridded macroclimate data (ERA5)

926 To make sure our macroclimate data obtained via the reference sensors outside the forest, did not
927 affect the temperature offset metrics (= temperature inside forest minus macroclimatic temperature
928 outside forests), we compared the macroclimatic temperature outside the forests determined with our
929 reference sensors with the ERA5-Land hourly data from the same period. ERA5 is a gridded
930 macroclimate layer at $0.1^\circ \times 0.1^\circ$ resolution and available for 1981 to present (Muñoz Sabater, 2019).

931 Macroclimatic data obtained from our reference sensors placed outside the forests correlated well
932 with gridded macroclimate data (ERA5) (**Figure C1**). We especially found warmer conditions in
933 maximum temperatures when the reference loggers outside the forests were used (as indicated by the
934 positive intercept in Figure C1). Since this is a very consistent and almost constant warming effect,
935 this is probably related to the passive radiation shield (i.e. insulating effect due to insufficient
936 ventilation and higher warming rates). However, irrespective of a possible bias, the same shield was
937 applied everywhere across all plots.

938 To check the sensitivity of our results, we also computed the offset based on the temperature data
939 from ERA5 instead of using the reference loggers and repeated the modelling with our design
940 variables as predictors and the mean, maximum and minimum temperature offset as responses.

941 Results can be found in **Table C1**. These sensitivity analyses confirm the robustness of our main
942 findings regarding the drivers of forest edge microclimate. We decided to use our own open-air
943 reference sensors to calculate all offsets for the main text analyses because these sensors were always
944 placed in the immediate vicinity of our forests and because such measurements have been shown to
945 be most reliable in forests (Maclean et al., 2021).



946

947 **Figure C1:** Comparison of the seasonal (summer, autumn, winter and spring) macroclimatic air temperatures using our reference
 948 sensors and the seasonal macroclimatic temperatures based on the ERA5-Land hourly data from the same period (Muñoz Sabater,
 949 2019). Dots represent the individual reference sensors, the colours represent the average seasonal maximum (red), mean (grey) or
 950 minimum (blue) temperature with in grey shaded their confidence intervals. Additionally, the 1:1 reference line is shown in black.

951 **Table C1:** Overview of the results of the linear mixed-effect models using the design variables (mean annual temperature (= MAT,
952 from the reference sensors), forest management type (= dense, intermediate or open) and distance to the edge and their interaction
953 effects on the mean, minimum and maximum air temperature offset during summer and winter, calculated using the ERA5-Land hourly
954 data as reference temperature data for the open area outside the forest. Dense forests were used as the reference management type. The
955 coefficient estimates of the models are given and the significance of the effect is indicated with asterisks (* = $p < 0.05$, ** = $p < 0.01$,
956 *** = $p < 0.001$).

	Summer mean air temperature offset (°C)	Winter mean air temperature offset (°C)	Summer max. air temperature offset (°C)	Winter max. air temperature offset (°C)	Summer min. air temperature offset (°C)	Winter min. air temperature offset (°C)
MAT (°C)	-0.97	-1.46 ***	-0.49	-	-1.02**	-1.59 ***
Intermediate forests	0.23	-	-	-	-	-
Open forests	0.58	-	-	-	-	-
Distance to the edge (m, log- transformed)	-0.08 *	-0.09 ***	-0.61 ***	-0.57 ***	0.11 ***	0.07 ***
MAT × Distance	0.06 *	-	0.28 *	-	0.05 **	0.03 *
MAT × Intermediate	-	-	-	-	-	-
MAT × Open	-	-	-	-	-	-
Intermediate × Distance	-0.03	-	-	-	-	-
Open × Distance	-0.14 *	-	-	-	-	-

957

958 References Appendix

- 959 Govaert, S., Meeussen, C., Vanneste, T., Bollmann, K., Brunet, J., Cousins, S.A.O., Diekmann, M., Graae, B.J.,
960 Hedwall, P.O., Heinken, T., Iacopetti, G., Lenoir, J., Lindmo, S., Orczewska, A., Perring, M.P., Ponette, Q., Plue,
961 J., Selvi, F., Spicher, F., Tolosano, M., Vermeir, P., Zellweger, F., Verheyen, K., Vangansbeke, P., De Frenne, P.,
962 2020. Edge influence on understorey plant communities depends on forest management. *J. Veg. Sci.* 31, 281–292.
963 <https://doi.org/10.1111/jvs.12844>
- 964 Maclean, I., Duffy, J., Haesen, S., Govaert, S., De Frenne, P., Vanneste, T., Lenoir, J., Lembrechts, J., Rhodes, J., Van
965 Meerbeek, K., 2021. On the measurement of microclimate. *Methods in Ecology and Evolution*.
966 <https://doi.org/10.1111/2041-210X.13627>
- 967
- 968 Muñoz Sabater, J., (2019): ERA5-Land hourly data from 1981 to present. Copernicus Climate Change Service (C3S)
969 Climate Data Store (CDS). (Accessed on 23-02-2021), <https://doi.org/10.24381/cds.e2161bac>
- 970 Verheyen, K., Baeten, L., De Frenne, P., Bernhardt-Römermann, M., Brunet, J., Cornelis, J., Decocq, G., Dierschke, H.,
971 Eriksson, O., Hédli, R., Heinken, T., Hermy, M., Hommel, P., Kirby, K., Naaf, T., Peterken, G., Petřík, P.,
972 Pfadenhauer, J., Van Calster, H., Walther, G.R., Wulf, M., Verstraeten, G., 2012. Driving factors behind the
973 eutrophication signal in understorey plant communities of deciduous temperate forests. *J. Ecol.* 100, 352–365.
974 <https://doi.org/10.1111/j.1365-2745.2011.01928.x>
- 975